

RAGE is a receptor for SARS-CoV-2 N protein and mediates N protein-induced acute lung injury

Jie Xia^{1†}, Jiangmei Wang^{1†}, Liyang Ying¹, Ruoqiong Huang¹, Kai Zhang², Ruoyang Zhang¹, Wenqi Tang¹, Qi Xu³, Dengming Lai¹, Yan Zhang¹, Yaoqin Hu¹, Xiaodie Zhang¹, Ruoxi Zang¹, Jiajie Fan¹, Qiang Shu^{1,*}, Jianguo Xu^{1,*}

¹The Children's Hospital of Zhejiang University School of Medicine and National Clinical Research Center for Child Health, 3333 Binsheng Road, Hangzhou, Zhejiang, 310052, China

²The First Affiliated Hospital of Zhejiang University School of Medicine, Hangzhou, Zhejiang, 310006, China

³Hangzhou Medical College, 182 Tianmu District, Hangzhou, Zhejiang, 310025, China

†These authors contributed equally to this work.

*Corresponding Authors:

Qiang Shu, Department of Thoracic and Cardiovascular Surgery, The Children's Hospital of Zhejiang University School of Medicine, 3333 Binsheng Road, Hangzhou, Zhejiang, 310052, China, shuqiang@zju.edu.cn

Jianguo Xu, Department of Thoracic and Cardiovascular Surgery, The Children's Hospital of Zhejiang University School of Medicine, 3333 Binsheng Road, Hangzhou, Zhejiang, 310052, China, jxu5@yahoo.com

Author contributions: JXia, JW, QS, and JXu conceived and designed the experiments; JXia, JW, LY, RH, KZ, RZ, WT, QX, DL, YZ, YH, XZ, RZ, JF performed the experiments; JXia, JW, LY, RH, KZ, RZ, WT, QX, DL, YZ, YH, XZ, RZ, JF, QS, JXu analyzed and interpreted the data; All authors involved in drafting the manuscript and approved the manuscript.

Sources of funding: This work was supported by the Natural Science Foundation of Zhejiang Province (Grant No. LQY19H190001), the Health Commission of Zhejiang Province (Grant No. 2021KY188), and the National Natural Science Foundation of China (Grant No. 81772122, 82070074, 82272191).

Running title: RAGE as a receptor for SARS-CoV-2 N protein

This article is open access and distributed under the terms of the Creative Commons Attribution Non-Commercial No Derivatives License 4.0 (<http://creativecommons.org/licenses/by-nc-nd/4.0/>). For commercial usage and reprints please contact Diane Gern (dgern@thoracic.org).

This article has an online data supplement, which is accessible from this issue's table of content online at www.atsjournals.org.

Abstract

SARS-CoV-2 nucleocapsid protein (N-protein) rises early in body fluids during infection and has recently been identified as a direct inducer for lung injury. However, the signal mechanism of N-protein in lung inflammatory response remains poorly understood. The goal of this study was to determine whether receptor for advanced glycation endproducts (RAGE) participated in N-protein-induced acute lung injury. The binding between N-protein and RAGE was examined via assays for protein-protein interaction. To determine the signaling mechanism *in vitro*, cells were treated with recombinant N-protein and assayed for the activation of RAGE/mitogen-activated protein kinase/NF- κ B pathway. RAGE deficiency mice and antagonist were applied to study N-protein-induced acute lung injury *in vivo*. Binding between N-protein and RAGE was confirmed via flow cytometry-based binding assay, surface plasmon resonance, and enzyme-linked immunosorbent assay. Pull-down and co-immunoprecipitation assays revealed that N-protein bound RAGE via both N-terminal and C-terminal domains. *In vitro*, N-protein activated RAGE-ERK1/2-NF- κ B signaling pathway and induced proinflammatory response. RAGE deficiency subdued N-protein-induced proinflammatory signaling and response. *In vivo*, RAGE was upregulated in the bronchioalveolar lavage and lung tissue after recombinant N-protein insult. RAGE deficiency and small molecule antagonist partially protected mice from N-protein-induced acute lung injury. Our study demonstrated that RAGE is a receptor for N-protein. RAGE is partially responsible for N-protein-induced acute lung injury and has the potential to become a therapeutic target for treating Coronavirus disease 2019.

Abstract word count: 224

Key words: SARS-CoV-2, receptor for advanced glycation endproducts, nucleocapsid protein, receptor, acute lung injury

Introduction

Coronavirus disease 2019 (COVID-19) pandemic, caused by infection of SARS-CoV-2, has resulted in profound public health and socioeconomic consequences around the globe (1). Acute lung injury and acute respiratory distress syndrome (ARDS) are the most serious and frequent complications of COVID-19. The mortality rate of COVID-19 ARDS is estimated to be about 45%, while the incidence of ARDS among COVID-19 non-survivors is approximately 90% (2). Both classical and COVID-19 ARDS are characterized by increased endothelial permeability, infiltration of inflammatory cells, and elevated proinflammatory cytokines such as interleukin (IL)-6, IL-8, and tumor necrosis factor (TNF)- α (3).

SARS-CoV-2 is an enveloped, positive sense, single-stranded RNA virus with a genome size of approximately 30,000 nucleotides. The virion envelop is anchored with three of the four structural proteins: the spike (S), the membrane (M), and the envelope (E) proteins (4). The fourth, the nucleocapsid protein (N-protein), is located inside of the viral envelope. It packages RNA genome into helical ribonucleoprotein complex enclosed within the capsid, which is essential for viral replication and infection (5). The N-protein is composed of two RNA-binding domains, the N-terminal domain (NTD) and C-terminal domain (CTD), which are connected by a Ser/Arg-rich linker region (LR) (6). Several studies have documented that SARS-CoV-2 N-protein is directly involved in lung inflammation and acute lung injury. Gao et al. reported that N-protein aggregated lipopolysaccharide (LPS)-induced lung injury via binding to MASP-2, leading to complement activation (7). Pan et al. found that N-protein boosted NLRP3 inflammasome activation to induce lung inflammation (8). Our results showed that recombinant N-protein induced acute lung injury in mice via NF- κ B activation

(9). However, the upstream mechanism of NF- κ B activation is unknown.

One of the upstream mediators of NF- κ B activation is receptor for advanced glycation endproducts (RAGE). RAGE is a transmembrane glycoprotein and belongs to the immunoglobulin superfamily. In addition to binding with advanced glycation endproducts, RAGE is also a receptor for many other ligands such as LPS, family of S100 proteins, and high mobility group box 1 (HMGB1) (10). Compared with other tissues, RAGE is most highly expressed in the lung, particularly in the alveolar type I cells, type II cells, and macrophages (11, 12). A potential role of RAGE in the pathogenesis of COVID-19 has been proposed by several groups (13). However, the role of RAGE in N-protein-induced acute lung injury has not been reported. In the present study, we aimed to examine whether RAGE is a receptor for N-protein and determine the consequent impact on acute lung injury of N-protein-RAGE interaction.

Methods

Detailed METHODS are provided in the online supplement.

Plasmids and fusion proteins

N-protein N-terminal domain (NTD, 1-174 AA), linker region (LR, 175-246 AA), and C-terminal domain (CTD, 247-419 AA) constructs were amplified from a full-length N-protein cDNA via PCR, confirmed via sequencing, and subcloned into pcDNA3.1-GFP plasmid in frame for mammalian expression. Human RAGE cDNA construct was amplified from a full-length RAGE cDNA via PCR, confirmed via sequencing, and subcloned into pcDNA3.1-Flag

plasmid. The construct for full-length pET28a-His-N-protein for bacterial expression was generously provided by Dr. Feng Cong from Guangdong Laboratory Animals Monitoring Institute. Recombinant His-protein constructs for NTD, LR, and CTD were amplified from an N-protein cDNA via PCR, confirmed via sequencing, and inserted into pET28a vector. Recombinant RAGE protein was purchased from SinoBiological (Beijing, China).

Preparation of recombinant N-protein

The proteins were purified from bacterial lysate via nickel affinity chromatography (BBI Life Sciences) and dialyzed to remove extra salt and imidazole. To remove the contaminated endotoxin, the recombinant proteins were passed through a column from ToxinEraser Endotoxin Removal Kit (GenScript). The endotoxin levels were < 0.1 EU/ μg protein (< 0.01 ng/ μg) as determined by ToxinSensor Chromogenic LAL Endotoxin Assay Kit (GenScript). To neutralize the possible protein-bound LPS, recombinant proteins were pretreated with polymyxin B (250 $\mu\text{g}/\text{ml}$, MilliporeSigma) for 1 h at room temperature (RT) before all in vitro and in vivo experiments.

Flow cytometry-based binding assay

Cells were detached by cell scrapers and rinsed with flow cytometry buffer (PBS, 0.5 % BSA) to block non-specific binding. Cells were then incubated with His-tagged full-length N-protein (5 $\mu\text{g}/\text{ml}$) at 37 °C for 1 h. Cells were washed with flow cytometry buffer for 3 x 5 min and incubated with an Alexa Fluor 488-conjugated anti-His antibody (Biolegend) diluted 1:100 for 30 min. Then, cells were rinsed, detected by a BD LSRFortessa™ flow cytometer, and analyzed using FlowJo V10 software.

Surface plasmon resonance (SPR)

SPR was performed using a Biacore 3000 system (Cytiva). N-protein was diluted in PBS

to generate a series of concentrations (6.25-400 nM). After immobilizing RAGE at 100 RU level on the surface of a CM5 sensor chip (Cytiva), N-protein samples were injected for 4 min across the sensor surface at a flow rate of 20 μ L/min. At the end of the sample injection, PBS was flowed over the sensor surface for 4 min to promote dissociation. The response was monitored as a function of time at RT. Sensorgrams were obtained by subtraction of zero concentration curve. The binding data was fitted to a 1:1 binding model using BIAevaluation software (Cytiva).

N-protein-induced lung injury model

C57BL/6 mice were acquired from Shanghai Laboratory Animal Center (Shanghai, China). RAGE knockout mice with C57BL/6 background was generated by Nanjing Biomedical Research Institute of Nanjing University via CRISPR/Cas9 technology (Project#: XM709828). Animal experimental protocols were approved by the Institutional Animal Care and Use Committee at Zhejiang University School of Medicine. Mice were anesthetized with an injection of phenobarbital (50 mg/kg) intraperitoneally. Acute lung injury was induced via intratracheal instillation of recombinant full-length N-protein (75 μ g per mouse in 50 μ L) as reported previously (9). To study the effect of RAGE inhibition on N-protein-induced lung injury, mice were subjected to intraperitoneal injection of RAGE antagonist RAP (50 or 100 μ g/mouse) 1 h before N-protein administration. Based on our experience, the optimal time point for assessing N-protein-induced lung injury was 24 h after insult. Serum, lung, and bronchioalveolar lavage (BAL) samples were harvested at 24 h from mouse groups (48 h for Supplemental Figure 1).

Western blot

Antibodies for phosphor-ERK1/2 and ERK1/2 were purchased from Abcam. Antibodies for phosphor-JNK1/2, JNK1/2, phosphor-p38, p38, phosphor-NF- κ B p65, and NF- κ B p65 were purchased from Cell Signaling Technology. Equal amount of cell lysates (30 μ g) were separated on 12% SDS-PAGE gels, transferred via polyvinylidene fluoride membranes, blocked in tris-buffered saline with Tween-20 containing 5% non-fat milk (blot buffer), and probed with the primary antibodies. After washing with blot buffer, membranes were incubated with specific secondary antibodies linked to horseradish peroxidase. Signal detection was conducted using enzyme-linked chemiluminescence kit. Blot images were analyzed by ImageJ software.

Statistical methods

Data are presented as mean \pm standard deviation of the mean (SD). Data normality was examined using the D'Agostino-Pearson Omnibus normality test, the Shapiro-Wilk normality test, or Kolmogorov-Smirnov test with Dallal-Wilkinson-Lilliefors corrected p value. Student's t test, one-way analysis of variance (ANOVA) with Tukey's post hoc test, or two-way ANOVA with Tukey's post hoc test was conducted for parametric values. In data sets with non-parametric values (Figure 2F and TNF- α of Figure 3B), Kruskal-Wallis test followed by Dunn's post hoc test was performed for analysis. Statistical analysis was conducted using the GraphPad Prism 8.0.2. Results were deemed significant if $p < 0.05$.

Results

RAGE is a receptor for N-protein

RAGE is constitutively expressed in A549 human alveolar epithelial cells (14). The first experiment was to test whether recombinant full-length N-protein could bind to the surface of A549 cells using flow cytometry-based binding assay. Detached cells were incubated with or without His-tagged N-proteins and then analyzed by flow cytometry after incubation with an anti-His antibody. The results suggested that N-protein bound with surface molecules of A549 cells (Figure 1A). To determine whether N-protein could specifically bind with RAGE on cell surface, bone marrow-derived macrophages (BMDMs) were isolated from RAGE knockout mice with C57BL/6 background (RAGE^{-/-}) and wild-type (WT) C57BL/6 mice. We observed that full-length N-protein bound BMDMs from WT mice, while the binding was substantially reduced in BMDMs from RAGE^{-/-} mice (Figure 1B). Surface plasmon resonance (SPR) analysis demonstrated that N-protein had a strong binding affinity with RAGE, with equilibrium dissociation constant (K_d) of 34.5 ± 10.6 nM (Figure 1C). It has been documented that the binding between receptor binding domain (RBD) of SARS-CoV-2 S protein and angiotensin-converting enzyme 2 (ACE2) has a K_d in the range of 6–133 nM (15). To demonstrate that RAGE possesses potent binding with N-protein, N-protein was coated on plates and the binding of various concentrations of RAGE was assayed via ELISA. The half-maximal effective concentration (EC₅₀) was 3.87 ± 0.57 μg/mL for N-protein (Figure 1D). Lopez et al. reported that ACE2 bound with RBD of SARS-CoV2 S protein with an EC₅₀ value of 13.5 μg/mL (16).

To provide more evidences for N-protein and RAGE association, His-tagged proteins expressing full-length, N-terminal domain (N-NTD), linker region (N-LR), and C-terminal

domain (N-CTD) (Figure 1E) were utilized in pull-down assay of mouse lung lysate. Full-length N-protein, N-NTD, and N-CTD were able to pull down considerable amount of RAGE as detected by Western blot, while N-LR did not show binding activity (Figure 1F). To confirm the physical association of N-protein and RAGE in a cellular context, constructs of GFP-N-protein and Flag-RAGE were expressed in HEK-293 cells either alone or in combination via transient transfection. When cell lysates were immunoprecipitated with an anti-FLAG antibody, the co-transfected full-length N-protein, N-NTD, and N-CTD, but not N-LR, was robustly co-immunoprecipitated (Figure 1G). These results indicate that N-protein has two binding sites for RAGE, one at CTD and the other at NTD. Similarly, it has been reported that HMGB1 has two RAGE-binding domains (17).

N-protein activates RAGE-ERK1/2-NF- κ B pathway

Previously, our group reported that recombinant N-protein induced lung injury and NF- κ B activation, independent of endotoxin (9). To investigate the upstream signaling mechanism of NF- κ B activation, RAW 264.7 macrophages were treated with recombinant full-length N-protein for a series of time points. Cell lysates were examined for the phosphorylation of mitogen-activated protein kinases (MAPK) (ERK1/2, p38 MAPK, and JNK1/2) via Western blot analysis. The results showed that phosphorylation of ERK1/2, p38 MAPK, and JNK1/2 was elevated in a time-dependent manner, reaching a peak between 30 min to 1 h (Figures 2A-2C). Pretreatment of cells with RAGE antagonist (RAP, 20 μ M) blocked N-protein-induced ERK1/2 activation, indicating that RAGE is upstream of ERK1/2 (Figure 2D). The phosphorylation of p38 MAPK and JNK1/2 evoked by N-protein was unaltered by RAGE antagonist, suggesting that the activation of p38 MAPK and JNK1/2 is independent of RAGE (Figures 2E-2F). This phenomenon is similar to a previous report that

S100B increased phosphorylation of p38 MAPK and JNK1/2 independent of RAGE (18). Compared with the phosphorylation pattern of MAPK induced by N-protein (Figures 2A-2C), NF- κ B p65 phosphorylation lasted longer, reaching a peak between 1 h to 4 h (Figure 2G). Similar to that of ERK1/2, N-protein-induced NF- κ B p65 phosphorylation was blocked by RAGE antagonist (Figure 2H). Furthermore, ERK1/2 inhibition (SCH772948, 500 nM) abolished the effect of N-protein on NF- κ B activation, suggesting ERK1/2 is upstream of NF- κ B (Figure 2I). These findings support that N protein induces signaling through RAGE-dependent activation of ERK1/2-NF- κ B pathway.

N-NTD and N-CTD mimic full-length N-protein in signaling and inflammatory response

It has been reported that HEK 293 cells do not express or express low levels of RAGE (19). To examine whether N-NTD and N-CTD could promote RAGE-mediated signaling, HEK 293 cells were transfected with Flag-tagged RAGE and stimulated without or with recombinant proteins expressing full-length, N-NTD, N-CTD, or N-LR (5 μ g/mL) for 30 min. Without stimulation, the phosphorylation of ERK1/2 and NF- κ B p65 as detected by Western blot was almost undetectable. Treatment with full-length N-protein, N-NTD, and N-CTD, but not N-LR, elevated the phosphorylation of ERK1/2 and NF- κ B p65 (Figure 3A). To study whether N-NTD and N-CTD could enhance RAGE-mediated inflammatory response, transfected HEK293 cells were stimulated without or with recombinant proteins expressing full-length, N-NTD, N-CTD, or N-LR (5 μ g/mL) for 24 h. Full-length N-protein, N-NTD, and N-CTD significantly elevated both mRNA expression (Figure 3B) and cellular

release (Figure 3C) of proinflammatory cytokines IL-1 β , IL-6, and TNF- α as determined by qRT-PCR and ELISA, respectively.

RAGE deficiency reduces N-protein-induced ERK1/2-NF- κ B signaling and proinflammatory response

To further explore the role of RAGE in N-protein-induced proinflammatory pathway, BMDMs were isolated from RAGE^{-/-} and WT C57BL/6 mice and treated with recombinant full-length N-protein for different time points. Compared with WT BMDMs, phosphorylation of ERK1/2 and NF- κ B p65 was abolished in RAGE^{-/-} BMDMs in response to N-protein (Figure 4A). Compared with WT, RAGE deficiency significantly decreased the effect of N-protein on mRNA expression and cellular release of IL-1 β , IL-6, and TNF- α at 24 h (Figure 4B). However, RAGE deficiency did not totally wipe out the proinflammatory effect of N-protein. To further support the role of ERK1/2 in regulation of N-protein-induced proinflammatory response, WT BMDMs were treated with ERK1/2 inhibitor (SCH772948, 500 nM) prior to N-protein insult. ERK1/2 inhibition significantly inhibited the mRNA expression and cellular release of proinflammatory cytokines IL-1 β , IL-6, and TNF- α at 24 h (Figure 4C). Taken together, these findings indicate that RAGE-ERK1/2-NF- κ B pathway is essential in N-protein-induced proinflammatory response.

RAGE deficiency and inhibition alleviate N-protein-induced acute lung injury

Previously, our group reported that recombinant N-protein-induced lung injury was dose-dependent. Intratracheal administration of a low dose of N-protein (3 μ g/mouse) failed to trigger acute lung injury at 24 h, while a high dose (75 μ g/mouse) had more pronounced

effect than a medium dose (15 $\mu\text{g}/\text{mouse}$) (9). To study whether N-protein induces RAGE expression in vivo, WT C57BL/6 mice were treated intratracheally with recombinant full-length N-protein (75 $\mu\text{g}/\text{mouse}$) or PBS. At 24 h, N-protein insult significantly increased RAGE levels in the bronchioalveolar lavage (BAL) and serum relative to the control in ELISA assay (Figure 5A). The treatment also elevated total RAGE mRNA levels in BAL cells (Figure 5B). In addition, lungs with N-protein insult showed extensive RAGE reactivity in immunohistochemistry (Figure 5C), indicating that N-protein upregulates both membrane and soluble RAGE.

To examine the role of RAGE in N-protein-induced acute lung injury, RAGE^{-/-} and WT C57BL/6 mice were treated intratracheally with recombinant full-length N-protein (75 $\mu\text{g}/\text{mouse}$) or PBS. Lung samples and BAL were harvested at 24 h. Treatment of N-protein elicited edema and higher cellularity in WT mice compared with control. However, inflammatory cell infiltration and septal thickening was remarkable less prominent in treated RAGE^{-/-} mice compared with WT mice (Figure 5D). Total protein levels, number of total cells, and number of neutrophils in the BAL were significantly reduced (by 42.4%, 49.5%, and 50.8 %, respectively) in treated RAGE^{-/-} versus WT mice (Figure 5E). Proinflammatory cytokines including IL-1 β , IL-6 and TNF- α in the BAL were substantially decreased (by 49.1%, 59.1%, and 43.7%, respectively) in treated RAGE^{-/-} mice versus WT mice (Figure 5F). However, lung injury was not totally abolished in RAGE^{-/-} mice compared with control (Figures 5E-5F). Reduced lung injury in treated RAGE^{-/-} versus WT mice was still observed at 48 h after N-protein insult. However, increased protein leakage in BAL was no longer present in treated RAGE^{-/-} mice versus control (Supplemental Figure 1). These results show

that N-protein-induced acute lung injury is partially protected by RAGE deficiency. Using a lentivirus-mediated N-protein expression system, Pan et al. reported that N-protein mediated NLRP3 inflammasome activation and prompted hyperinflammation in the lung (8).

Intraabdominal administration of NLRP3 inhibitor MCC950 (10 mg/kg) alleviated lung injury induced by recombinant N-protein (Supplemental Figure 2), indicating NLRP3 activation is also partially responsible for N-protein-induced acute lung injury.

To determine the therapeutic potential of RAGE inhibition in N-protein-induced lung injury, C57BL/6 mice were treated with recombinant full-length N-protein intratracheally (75 µg/mouse), N-protein + RAGE antagonist RAP (100 µg/mouse intraperitoneally 1 h before N-protein insult), or PBS. RAGE inhibition alleviated the effect of N-protein on lung pathology (Figure 6A). It also significantly reduced total protein concentration (by 51.1%), total cell count (by 49.1%), and neutrophil infiltration (by 51.2 %) in the BAL (Figure 6B). Proinflammatory cytokines including IL-1 β , IL-6, and TNF- α in the BAL were significantly decreased (by 53.1%, 62.6%, and 45.2%, respectively) by RAGE inhibition (Figure 6C). RAGE inhibition with a lower dose of RAP (50 µg/mouse) had similar effect as the 100 µg dose in alleviating protein leakage in the BAL while failing to reduce neutrophil infiltration (Supplemental Figure 3). Several studies have reported that RAGE ligands such as S100A8 and S100A9 were upregulated in COVID-19 patients (20). S100A8 and S100A9 were shown to exacerbate lung inflammation via neutrophil accumulation in tuberculosis (21). Our results revealed that N-protein had similar effect as S100A8 and A9 in inducing acute lung injury (Supplemental Figure 4). These findings suggest RAGE inhibition might be beneficial in alleviating lung injury from both N-protein and other RAGE agonists in COVID-19.

Discussion

It has been well established that the association between SARS-CoV-2 S protein and ACE2 mediates the viral entry to cells. To our knowledge, this is the first study to report the binding between N-protein and RAGE, linking the second SARS-CoV-2 structural protein with a membrane receptor. This conclusion is substantiated by the following findings. (1) There was a direct high-affinity physical association between N-protein and RAGE (Figure 1A-1D). (2) N-protein bound RAGE via both N-terminal domain and C-terminal domains (Figure 1F-1G). (3) N-protein activated ERK1/2-NF- κ B pathway through RAGE (Figure 2). (4) N-NTD and N-CTD mimicked full-length N-protein to induce inflammatory response (Figure 3). (5) Genetic deletion of RAGE significantly decreased N-protein-induced signaling and proinflammatory response in vitro (Figure 4A-4B). (6) In mice, N-protein treatment elevated RAGE levels in the BAL and lung (Figure 5A-5C). (7) RAGE deficiency protected against N-protein-induced acute lung injury in mice (Figure 5E-5F). (8) Inhibition of RAGE signaling via antagonist significantly alleviated N-protein-induced acute lung injury (Figure 6).

Previously, our group reported that N-protein induced acute lung injury in mice via activation of NF- κ B (9). We speculated that a membrane receptor may mediate the binding with N-protein and activation of NF- κ B. In the preliminary experiments using pull-down and co-immunoprecipitation assays, we found that N-protein was unable to physically associate with Toll-like receptor 4, the receptor for LPS (data not shown). Then, we turned our attention to explore the binding between N-protein to RAGE. Our results demonstrated that NTD and CTD of N-protein, but not LR, bound with RAGE. Similarly, HMGB1 has two

RAGE-binding domains, one in the box A domain (23–50 AA) (22) and the other in the box B domain (150–183 AA) (23). It has been documented that both NTD and CTD of N-protein possess the ability of RNA binding (24). The presence of two domains with similar functions may help to reinforce the activation of RAGE-mediated signaling pathway. However, we did not examine the ligand-binding domains for N-protein in RAGE. The mature human RAGE is a glycoprotein with 404 amino acids. It consists of an extracellular domain (1–342 AA), a single transmembrane domain (amino acids 343–363), and a cytoplasmic tail (amino acids 364–404). The extracellular part consists of one variable domain (V) and two constant domains (C1 and C2). The majority of binding studies showed that ligands bind with V domain of RAGE, however the C1 domain also participates in the recognition of ligands (25). The molecular mechanism underlying the binding between N-protein and RAGE warrants further investigation.

The association between RAGE and COVID-19 has been reported in the literature. Lim et al. showed that serum sRAGE is a biomarker for predicting disease severity of COVID-19 and the need for mechanical ventilation (26). mRNA and protein levels of RAGE ligands such as S100A8, S100A9, S100A11, S100A12, and S100 P were significantly higher in the lung of COVID-19 fatal cases compared with healthy controls (27). Serum S100B levels were elevated in COVID-19 patients and correlated with disease severity (28). In addition, serum levels of S100A8/A9 and HMGB1 at admission had prognostic value for ICU admission and hospital death in COVID-19 patients (20). Furthermore, Jessop et al. found that RAGE antagonist improved the survival of SARS-CoV-2 infected mice and alleviated

lung inflammation and perivascular pathology (29). The present study brings new light to the role of RAGE in COVID-19.

Using immunohistochemistry, Massoth et al. found that N-protein localized predominantly extracellularly and within hyaline membrane in a big percentage of patients died of COVID-19 (3). During SARS-CoV-2 infection, N-protein can be released into extracellular space and blood via several mechanisms. First, N-protein can be naturally secreted from SARS-COV-2-infected cells. When transfected alone in HEK 293 cells, N-protein and S protein, but not E and M proteins, were readily detected in the cell lysate (30). Secondly, several studies showed that SARS-CoV-2 infection induced cell necrosis, leading to passive release of virions, viral proteins, cytoplasmic components into extracellular space and blood (31). Thirdly, one report showed that extracellular vesicles carrying S protein were generated by host cells and budded from the plasma membrane, indicating that N-protein might also be released via the same machinery (32). Clinical studies showed that serum N-protein concentration was closely correlated to disease severity and had a peak value from 1 ng/ml to 2.7 μ g/ml in COVID-19 patients (33, 34). The present study revealed that N-protein activated membrane receptor RAGE on target cells and mediated inflammatory response, providing the mechanism of N-protein in SARS-CoV-2-induced lung injury.

In the present study, inhibition or knockout of RAGE did not completely abolish the effects of N-protein on acute lung injury, which suggests that N-protein may have other binding partners. It has been reported that N-protein interacted directly with NLRP3 and promoted NLRP3 inflammasome activation to induce inflammatory response in the lung (8). Here we showed that N-protein-induced lung injury was partially blocked by NLRP3

inhibitor MCC950. Another study showed that N-protein bound with Smad3 and enhanced TGF- β /Smad3 signaling to induce acute kidney via G1 cell cycle arrest mechanism (35).

Moreover, interaction between N-protein and α -synuclein accelerated amyloid formation and cell death, which might explain the reported correlation between COVID-19 and Parkinsonism (36).

There are also a couple of findings worth mentioning. In the SDS-PAGE analysis, we noticed that N-NTD migrated slightly slower than the predicted 20 kDa, while the N-CTD (also expected 20 kDa) moved even slower than NTD (Figure 1D). The same phenomenon was also seen in the report from Nakayama et al (37). This finding suggests that N-NTD and N-CTD have differences in post-translation modification. Secondly, our study demonstrated that N-protein induced activation of ERK1/2, p38 MAPK, and JNK1/2. However, the activation of p38 MAPK and JNK1/2 was not affected by RAGE inhibition, suggesting that this effect is independent of RAGE. Ishihara et al. found that RAGE bound specifically with ERK but not with JNK or p38 MAPK (38). Somensi et al. documented that heat shock protein 70 induced activation of ERK1/2, p38 MAPK, and JNK. However only ERK1/2 activation was blocked by RAGE knockdown (39).

In conclusion, the present study reveals that RAGE is a cell surface receptor for N-protein. N-protein activates RAGE-ERK1/2-NF- κ B pathway and promotes the production of proinflammatory cytokines. N-protein-induced acute lung injury is partially mediated by RAGE. Therapeutic interventions targeting at RAGE may alleviate cytokine storm and ARDS in COVID-19.

References

1. Miller IF, Becker AD, Grenfell BT, Metcalf CJE. Disease and healthcare burden of COVID-19 in the United States. *Nat Med* 2020; 26: 1212-1217.
2. Tzotzos SJ, Fischer B, Fischer H, Zeitlinger M. Incidence of ARDS and outcomes in hospitalized patients with COVID-19: a global literature survey. *Crit Care* 2020; 24: 516.
3. Massoth LR, Desai N, Szabolcs A, Harris CK, Neyaz A, Crotty R, Chebib I, Rivera MN, Sholl LM, Stone JR, Ting DT, Deshpande V. Comparison of RNA In Situ Hybridization and Immunohistochemistry Techniques for the Detection and Localization of SARS-CoV-2 in Human Tissues. *Am J Surg Pathol* 2021; 45: 14-24.
4. V'Kovski P, Kratzel A, Steiner S, Stalder H, Thiel V. Coronavirus biology and replication: implications for SARS-CoV-2. *Nat Rev Microbiol* 2021; 19: 155-170.
5. EA JA, Jones IM. Membrane binding proteins of coronaviruses. *Future Virol* 2019; 14: 275-286.
6. Ribeiro-Filho HV, Jara GE, Batista FAH, Schleder GR, Costa Tonoli CC, Soprano AS, Guimaraes SL, Borges AC, Cassago A, Bajgelman MC, Marques RE, Trivella DBB, Franchini KG, Figueira ACM, Benedetti CE, Lopes-de-Oliveira PS. Structural dynamics of SARS-CoV-2 nucleocapsid protein induced by RNA binding. *PLoS Comput Biol* 2022; 18: e1010121.
7. Gao T, Zhu L, Liu H, Zhang X, Wang T, Fu Y, Li H, Dong Q, Hu Y, Zhang Z, Jin J, Liu Z, Yang W, Liu Y, Jin Y, Li K, Xiao Y, Liu J, Zhao H, Liu Y, Li P, Song J, Zhang L, Gao Y, Kang S, Chen S, Ma Q, Bian X, Chen W, Liu X, Mao Q, Cao C. Highly pathogenic coronavirus N protein aggravates inflammation by MASP-2-mediated lectin complement pathway overactivation. *Signal Transduct Target Ther* 2022; 7: 318.
8. Pan P, Shen M, Yu Z, Ge W, Chen K, Tian M, Xiao F, Wang Z, Wang J, Jia Y, Wang W, Wan P, Zhang J, Chen W, Lei Z, Chen X, Luo Z, Zhang Q, Xu M, Li G, Li Y, Wu J. SARS-CoV-2 N protein promotes NLRP3 inflammasome activation to induce hyperinflammation. *Nat Commun* 2021; 12: 4664.
9. Xia J, Tang W, Wang J, Lai D, Xu Q, Huang R, Hu Y, Gong X, Fan J, Shu Q, Xu J. SARS-CoV-2 N Protein Induces Acute Lung Injury in Mice via NF- κ B Activation. *Front Immunol* 2021; 12: 791753.
10. Pickering RJ, Tikellis C, Rosado CJ, Tsorotes D, Dimitropoulos A, Smith M, Huet O, Seeber RM, Abhayawardana R, Johnstone EK, Golledge J, Wang Y, Jandeleit-Dahm KA, Cooper ME, Pflieger KD, Thomas MC. Transactivation of RAGE mediates angiotensin-induced inflammation and atherogenesis. *J Clin Invest* 2019; 129: 406-421.
11. Fehrenbach H, Kasper M, Tschernig T, Shearman MS, Schuh D, Muller M. Receptor for advanced glycation endproducts (RAGE) exhibits highly differential cellular and subcellular localisation in rat and human lung. *Cell Mol Biol (Noisy-le-grand)* 1998; 44: 1147-1157.
12. Katsuoka F, Kawakami Y, Arai T, Imuta H, Fujiwara M, Kanma H, Yamashita K. Type II alveolar epithelial cells in lung express receptor for advanced glycation end products

- (RAGE) gene. *Biochem Biophys Res Commun* 1997; 238: 512-516.
13. Chiappalupi S, Salvadori L, Vukasinovic A, Donato R, Sorci G, Riuzzi F. Targeting RAGE to prevent SARS-CoV-2-mediated multiple organ failure: Hypotheses and perspectives. *Life Sci* 2021; 272: 119251.
 14. Pouwels SD, Hesse L, Wu X, Allam V, van Oldeniel D, Bhiekhari LJ, Phipps S, Oliver BG, Gosens R, Sukkar MB, Heijink IH. LL-37 and HMGB1 induce alveolar damage and reduce lung tissue regeneration via RAGE. *Am J Physiol Lung Cell Mol Physiol* 2021; 321: L641-L652.
 15. Barton MI, MacGowan SA, Kutuzov MA, Dushek O, Barton GJ, van der Merwe PA. Effects of common mutations in the SARS-CoV-2 Spike RBD and its ligand, the human ACE2 receptor on binding affinity and kinetics. *Elife* 2021; 10.
 16. Lopez E, Haycroft ER, Adair A, Mordant FL, O'Neill MT, Pymm P, Redmond SJ, Lee WS, Gherardin NA, Wheatley AK, Juno JA, Selva KJ, Davis SK, Grimley SL, Harty L, Purcell DF, Subbarao K, Godfrey DI, Kent SJ, Tham WH, Chung AW. Simultaneous evaluation of antibodies that inhibit SARS-CoV-2 variants via multiplex assay. *JCI Insight* 2021; 6.
 17. Yang H, Liu H, Zeng Q, Imperato GH, Addorisio ME, Li J, He M, Cheng KF, Al-Abed Y, Harris HE, Chavan SS, Andersson U, Tracey KJ. Inhibition of HMGB1/RAGE-mediated endocytosis by HMGB1 antagonist box A, anti-HMGB1 antibodies, and cholinergic agonists suppresses inflammation. *Mol Med* 2019; 25: 13.
 18. Tsoporis JN, Izhar S, Leong-Poi H, Desjardins JF, Huttunen HJ, Parker TG. S100B interaction with the receptor for advanced glycation end products (RAGE): a novel receptor-mediated mechanism for myocyte apoptosis postinfarction. *Circ Res* 2010; 106: 93-101.
 19. Raucci A, Cugusi S, Antonelli A, Barabino SM, Monti L, Bierhaus A, Reiss K, Saftig P, Bianchi ME. A soluble form of the receptor for advanced glycation endproducts (RAGE) is produced by proteolytic cleavage of the membrane-bound form by the sheddase a disintegrin and metalloprotease 10 (ADAM10). *FASEB J* 2008; 22: 3716-3727.
 20. Chen L, Long X, Xu Q, Tan J, Wang G, Cao Y, Wei J, Luo H, Zhu H, Huang L, Meng F, Huang L, Wang N, Zhou X, Zhao L, Chen X, Mao Z, Chen C, Li Z, Sun Z, Zhao J, Wang D, Huang G, Wang W, Zhou J. Elevated serum levels of S100A8/A9 and HMGB1 at hospital admission are correlated with inferior clinical outcomes in COVID-19 patients. *Cell Mol Immunol* 2020; 17: 992-994.
 21. Gopal R, Monin L, Torres D, Slight S, Mehra S, McKenna KC, Fallert Junecko BA, Reinhart TA, Kolls J, Baez-Saldana R, Cruz-Lagunas A, Rodriguez-Reyna TS, Kumar NP, Tessier P, Roth J, Selman M, Becerril-Villanueva E, Baquera-Heredia J, Cumming B, Kasprovicz VO, Steyn AJ, Babu S, Kaushal D, Zuniga J, Vogl T, Rangel-Moreno J, Khader SA. S100A8/A9 proteins mediate neutrophilic inflammation and lung pathology during tuberculosis. *Am J Respir Crit Care Med* 2013; 188: 1137-1146.
 22. LeBlanc PM, Doggett TA, Choi J, Hancock MA, Durocher Y, Frank F, Nagar B, Ferguson TA, Saleh M. An immunogenic peptide in the A-box of HMGB1 protein reverses apoptosis-induced tolerance through RAGE receptor. *J Biol Chem* 2014; 289:

- 7777-7786.
23. Huttunen HJ, Fages C, Kuja-Panula J, Ridley AJ, Rauvala H. Receptor for advanced glycation end products-binding COOH-terminal motif of amphoterin inhibits invasive migration and metastasis. *Cancer Res* 2002; 62: 4805-4811.
 24. Chauhan A, Avti P, Shekhar N, Prajapat M, Sarma P, Bhattacharyya A, Kumar S, Kaur H, Prakash A, Medhi B. Structural and conformational analysis of SARS CoV 2 N-CTD revealing monomeric and dimeric active sites during the RNA-binding and stabilization: Insights towards potential inhibitors for N-CTD. *Comput Biol Med* 2021; 134: 104495.
 25. Fritz G. RAGE: a single receptor fits multiple ligands. *Trends Biochem Sci* 2011; 36: 625-632.
 26. Lim A, Radujkovic A, Weigand MA, Merle U. Soluble receptor for advanced glycation end products (sRAGE) as a biomarker of COVID-19 disease severity and indicator of the need for mechanical ventilation, ARDS and mortality. *Ann Intensive Care* 2021; 11: 50.
 27. Wu M, Chen Y, Xia H, Wang C, Tan CY, Cai X, Liu Y, Ji F, Xiong P, Liu R, Guan Y, Duan Y, Kuang D, Xu S, Cai H, Xia Q, Yang D, Wang MW, Chiu IM, Cheng C, Ahern PP, Liu L, Wang G, Surana NK, Xia T, Kasper DL. Transcriptional and proteomic insights into the host response in fatal COVID-19 cases. *Proc Natl Acad Sci U S A* 2020; 117: 28336-28343.
 28. Aceti A, Margarucci LM, Scaramucci E, Orsini M, Salerno G, Di Sante G, Gianfranceschi G, Di Liddo R, Valeriani F, Ria F, Simmaco M, Parnigotto PP, Vitali M, Romano Spica V, Michetti F. Serum S100B protein as a marker of severity in Covid-19 patients. *Sci Rep* 2020; 10: 18665.
 29. Jessop F, Schwarz B, Scott D, Roberts LM, Bohrnsen E, Hoidal JR, Bosio CM. Impairing RAGE signaling promotes survival and limits disease pathogenesis following SARS-CoV-2 infection in mice. *JCI Insight* 2022; 7.
 30. Plescia CB, David EA, Patra D, Sengupta R, Amiar S, Su Y, Stahelin RV. SARS-CoV-2 viral budding and entry can be modeled using BSL-2 level virus-like particles. *J Biol Chem* 2021; 296: 100103.
 31. Morais da Silva M, Lira de Lucena AS, Paiva Junior SSL, Florencio De Carvalho VM, Santana de Oliveira PS, da Rosa MM, Barreto de Melo Rego MJ, Pitta M, Pereira MC. Cell death mechanisms involved in cell injury caused by SARS-CoV-2. *Rev Med Virol* 2021: e2292.
 32. Verta R, Grange C, Skovronova R, Tanzi A, Peruzzi L, Deregibus MC, Camussi G, Bussolati B. Generation of Spike-Extracellular Vesicles (S-EVs) as a Tool to Mimic SARS-CoV-2 Interaction with Host Cells. *Cells* 2022; 11.
 33. Zhang Y, Ong CM, Yun C, Mo W, Whitman JD, Lynch KL, Wu AHB. Diagnostic Value of Nucleocapsid Protein in Blood for SARS-CoV-2 Infection. *Clin Chem* 2021.
 34. Pollock NR, Savage TJ, Wardell H, Lee RA, Mathew A, Stengelin M, Sigal GB. Correlation of SARS-CoV-2 Nucleocapsid Antigen and RNA Concentrations in Nasopharyngeal Samples from Children and Adults Using an Ultrasensitive and Quantitative Antigen Assay. *J Clin Microbiol* 2021; 59.
 35. Wang W, Chen J, Hu D, Pan P, Liang L, Wu W, Tang Y, Huang XR, Yu X, Wu J, Lan

- HY. SARS-CoV-2 N Protein Induces Acute Kidney Injury via Smad3-Dependent G1 Cell Cycle Arrest Mechanism. *Adv Sci (Weinh)* 2022; 9: e2103248.
36. Semerdzhiev SA, Fakhree MAA, Segers-Nolten I, Blum C, Claessens M. Interactions between SARS-CoV-2 N-Protein and alpha-Synuclein Accelerate Amyloid Formation. *ACS Chem Neurosci* 2022; 13: 143-150.
37. Nakayama EE, Kubota-Koketsu R, Sasaki T, Suzuki K, Uno K, Shimizu J, Okamoto T, Matsumoto H, Matsuura H, Hashimoto S, Tanaka T, Harada H, Tomita M, Kaneko M, Yoshizaki K, Shioda T. Anti-nucleocapsid antibodies enhance the production of IL-6 induced by SARS-CoV-2 N protein. *Sci Rep* 2022; 12: 8108.
38. Ishihara K, Tsutsumi K, Kawane S, Nakajima M, Kasaoka T. The receptor for advanced glycation end-products (RAGE) directly binds to ERK by a D-domain-like docking site. *FEBS Lett* 2003; 550: 107-113.
39. Somensi N, Brum PO, de Miranda Ramos V, Gasparotto J, Zanotto-Filho A, Rostirolla DC, da Silva Morrone M, Moreira JCF, Pens Gelain D. Extracellular HSP70 Activates ERK1/2, NF-kB and Pro-Inflammatory Gene Transcription Through Binding with RAGE in A549 Human Lung Cancer Cells. *Cell Physiol Biochem* 2017; 42: 2507-2522.

Acknowledgements

The construct of His-tagged N-protein of SARS-CoV-2 was a kind gift from Dr. Feng Cong, Guangdong Laboratory Animals Monitoring Institute, China.

Figure legends

Figure 1. N-protein bound to RAGE. (A) Detached A549 cells were incubated with or without His-tagged full-length N-protein under unpermeabilized condition for 1 h and washed with PBS + 0.5% BSA for 3 times. Binding of N-protein to A549 cells was measured by flow cytometry using an Alexa Fluor 488-conjugated anti-His antibody. (B) Detached BMDMs from RAGE^{-/-} and WT C57BL/6 mice were incubated with or without His-tagged full-length N-protein under unpermeabilized condition for 1 h and washed with PBS + 0.5% BSA for 3 times. Binding of N-protein to BMDMs was measured by flow cytometry using an Alexa Fluor 488-conjugated anti-His antibody. (C) SPR sensorgrams showed the binding of immobilized RAGE to N-protein at concentrations of 400, 200, 100, 50, 25, 12.5 and 6.25 nM. The data was fitted to the one-to-one kinetic model. (D) Recombinant RAGE of different concentrations (0.1 - 25.6 µg/ml) was applied to ELISA plates coated with N-protein. Bound RAGE was detected using a rabbit anti-RAGE antibody followed by a goat anti-rabbit secondary antibody conjugated to horseradish peroxidase. After adding substrate, optical density (OD) was measured at 450 nm and normalized against negative control. (E) A schematic diagram showed full-length and truncated N-proteins. (F) Lung lysates were prepared from C57BL/6 mice and pulled down with His-tagged full-length N-protein, N-NTD, N-CTD, or N-LR. The lysates and pull-down products were examined via Western blot using an anti-RAGE antibody. The two bands detected in the pull-down assay represent the RAGE protein pre and post glycosylation (upper panel). Bait proteins were visualized with Coomassie staining (lower panel). (G) Cell lysates from HEK 293 cells expressing FLAG-RAGE and GFP-N-proteins of full-length, N-NTD, N-CTD, or N-LR were subjected to immunoprecipitation using an anti-FLAG antibody. The cell lysates and immunoprecipitation

fractions were examined by Western blot using an anti-GFP or anti-Flag antibody. Data are presented as mean \pm SD (D). Data shown are representative of three independent experiments.

Figure 2. N-protein prompted ERK-mediated NF- κ B phosphorylation via RAGE. (A-C) RAW 264.7 cells were treated with recombinant full-length N-protein (5 μ g/mL) for the indicated times. Cell lysates were analyzed via Western blot using antibodies specific to phosphorylated (upper panels) or total (lower panels) of ERK1/2 (A), p38 MAPK (B), or JNK1/2 (C). (D-F) RAW 264.7 cells were pretreated with RAGE antagonist (RAP, 20 μ M) for 1 h and then incubated with recombinant full-length N-protein (5 μ g/mL) for the indicated times. Cell lysate was examined via Western blot using specific antibodies to detect phosphorylation of ERK1/2 (D), p38 MAPK (E), or JNK1/2 (F). (G-H) RAW 264.7 cells were pretreated without (G) or with (H) RAGE antagonist RAP (20 μ M) for 1 h and then stimulated with recombinant full-length N-protein (5 μ g/mL) for the indicated times. Cell lysate was assessed via Western blot using antibodies specific to phospho-NF- κ B p65 (upper panel) or total NF- κ B p65 (lower panel). (I) RAW 264.7 cells were pretreated with ERK inhibitor (SCH772948, 500 nM) for 1 h and then stimulated with recombinant full-length N-protein (5 μ g/mL) for the indicated times. Cell lysate was examined via Western blot using antibodies specific to phospho-NF- κ B p65 (upper panel) or total NF- κ B p65 (lower panel). N-protein for all groups was pretreated with polymyxin B (250 μ g/ml) for 1 h at RT before all experiments to neutralize endotoxin. The band density of phosphorylation was quantified with ImageJ software, normalized to that of total protein, and expressed as relative fold

change compared with time 0. Data are presented as mean \pm SD, $n = 3$. * $p < 0.05$, ** $p < 0.01$, *** $p < 0.001$ versus time 0. One-way analysis of variance with Tukey's post hoc test (A-E, G-I) or Kruskal-Wallis test with Dunn's post hoc test (F) was used for the analysis. NS: not significant. n: number of independent experiments.

Figure 3. N-NTD and N-CTD induced proinflammatory signaling and immune response. (A) HEK293 cells were transiently transfected with RAGE for 24 h and treated with recombinant N-proteins expressing full-length, N-NTD, N-CTD, or N-LR (5 $\mu\text{g}/\text{mL}$) for 30 min. Cell lysates were analyzed via Western blot using antibodies specific to phosphorylated (upper panels) or total (lower panels) of ERK1/2 or NF- κB p65. The levels of phosphorylation were quantified with ImageJ software ($n = 3$). (B-C) HEK293 cells were transiently transfected with RAGE for 24 h and treated with recombinant proteins expressing full-length, NTD, CTD, or LR of N-protein (5 $\mu\text{g}/\text{mL}$) for 24 h. (B) The mRNA expression of proinflammatory cytokines IL-1 β , IL-6, and TNF- α in HEK293 cells was quantitated by qRT-PCR ($n = 8-9$). (C) Culture supernatants were analyzed by ELISA for IL-1 β , IL-6, and TNF- α ($n = 6$). Data are presented as mean \pm SD. * $p < 0.05$, ** $p < 0.01$, *** $p < 0.001$ versus no N-protein treatment. One-way analysis of variance with Tukey's post hoc test (A, B and C, except B-TNF- α) or Kruskal-Wallis test with Dunn's post hoc test (B-TNF- α) was used for the analysis. NS: not significant. n: number of independent experiments.

Figure 4. RAGE knockout reduced inflammatory response induced by N-protein in BMDMs.

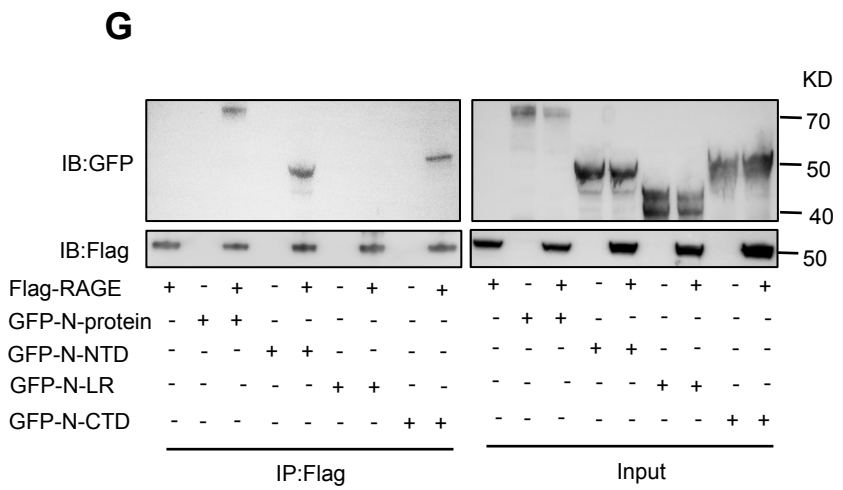
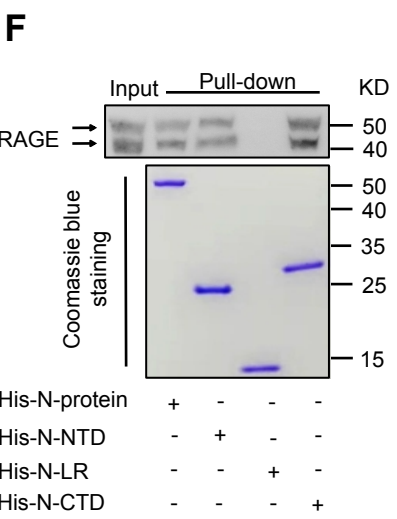
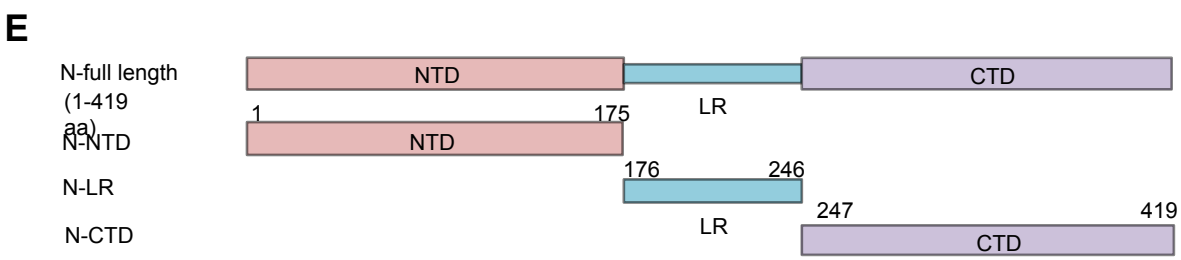
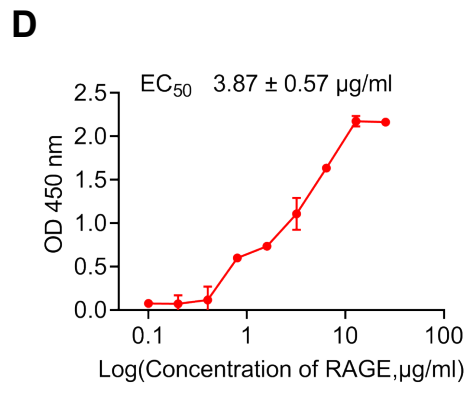
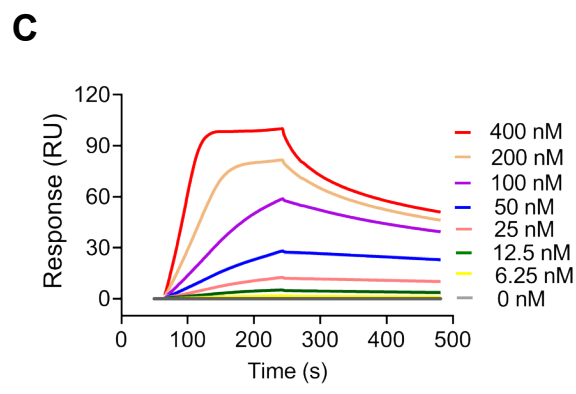
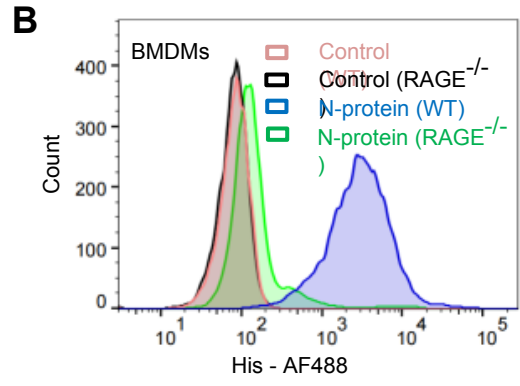
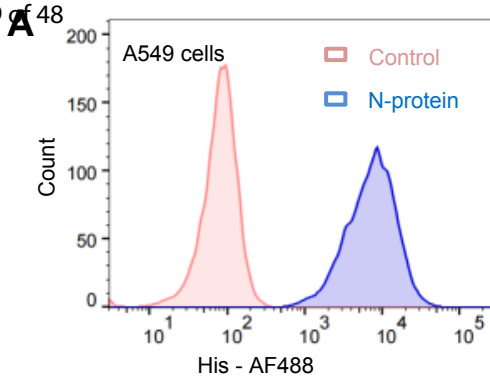
(A) BMDMs from WT and RAGE knockout mice were treated with recombinant full-length

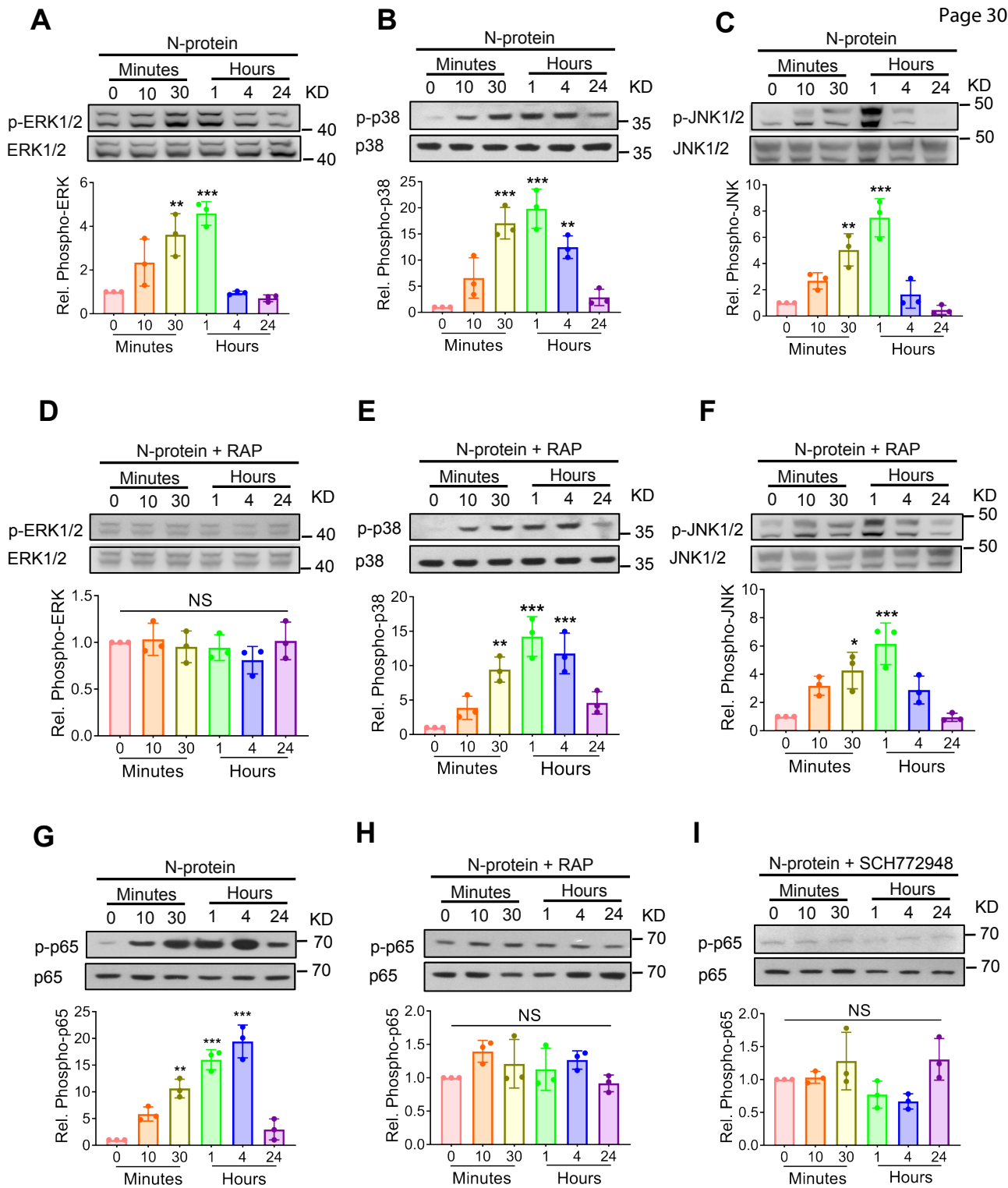
N-protein (5 $\mu\text{g}/\text{mL}$) for the indicated times. Cell lysate was analyzed via Western blot using antibodies specific to phosphorylated (upper panels) or total (lower panels) of ERK1/2 or NF- κB p65. The levels of phosphorylation were quantified with ImageJ software (n = 3). (B) BMDMs from WT and RAGE knockout mice were treated with N-protein (5 $\mu\text{g}/\text{mL}$) for 24 h. The mRNA expression of proinflammatory cytokines IL-1 β , IL-6, and TNF- α in BMDMs was quantitated by qRT-PCR (upper panel, n = 6). Culture supernatants were analyzed by ELISA for IL-1 β , IL-6, and TNF- α (lower panel, n = 6). (C) BMDMs from WT mice were pretreated with ERK1/2 inhibitor (SCH772948, 500 nM) for 1 h and then stimulated with recombinant N-protein (5 $\mu\text{g}/\text{mL}$) for 24 h. The mRNA expression of proinflammatory cytokines IL-1 β , IL-6, and TNF- α was quantitated by qRT-PCR (upper panel, n = 9). Culture supernatants were analyzed by ELISA for IL-1 β , IL-6, and TNF- α (lower panel, n = 6). Data are presented as mean \pm SD. *p < 0.05, **p < 0.01, ***p < 0.001. One-way AVOVA with Tukey's post hoc test versus time 0 (A). Two-way AVOVA with Tukey's post hoc test (B). One-way AVOVA with Tukey's post hoc test (C). NS: not significant. n: number of independent experiments.

Figure 5. RAGE mediated N-protein-induced acute lung injury. (A-C) WT C57BL/6 mice were administered intratracheally with His-tagged full-length N-protein (75 $\mu\text{g}/\text{mouse}$ in 50 μl) or PBS. (A) BAL and serum samples were harvested at 24 h. RAGE levels in the BAL and serum were determined by ELISA (n = 8). (B) Total RAGE mRNA expression in BAL cells was examined via qRT-PCR (n = 9). (C) RAGE expression in lung tissue was detected via immunohistochemistry (n = 3). (D-F) RAGE^{-/-} mice with C57BL/6 background and WT

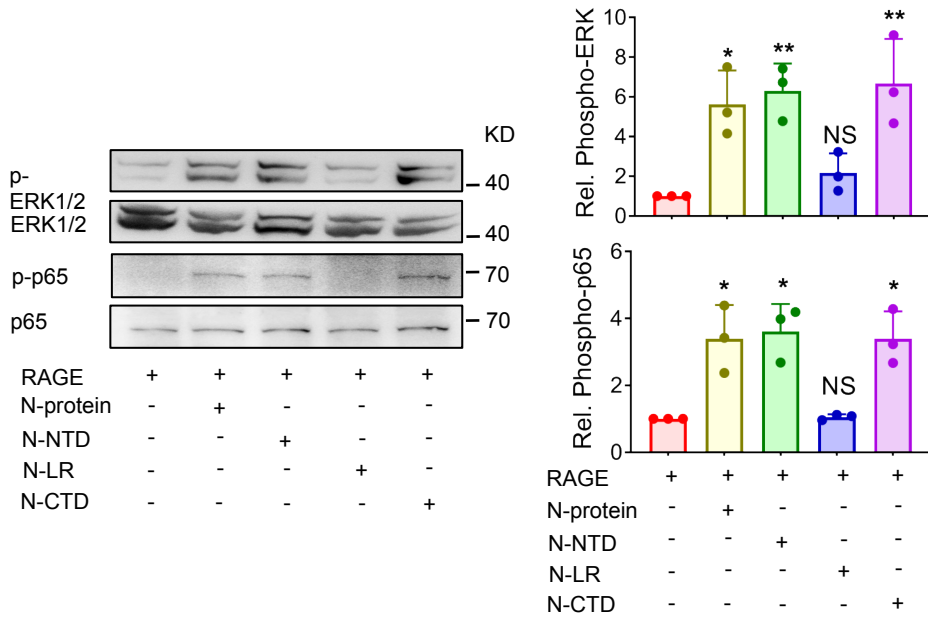
C57BL/6 mice were treated with PBS or N-protein (75 $\mu\text{g}/\text{mouse}$ in 50 μl) intratracheally. Lung tissue and BAL samples were collected at 24 h after N-protein insult. (D) Tissue sections were stained with H&E (n = 3). (E) Total protein, total cells, and neutrophils in the BAL were assayed to evaluate lung injury (n = 8). (F) Levels of IL-1 β , IL-6, and TNF- α in the BAL were determined via ELISA (n = 8). Data are presented as mean \pm SD. **p < 0.01, ***p < 0.001. Student's two-tailed t test (A-B). Two-way AVOVA with Tukey's post hoc test (E-F). NS: not significant. n: number of independent experiments.

Figure 6. RAGE antagonist reduced N-protein-induced acute lung injury. (A-C) WT C57BL/6 mice were treated with PBS, full-length N-protein (75 $\mu\text{g}/\text{mouse}$), or N-protein + RAGE antagonist RAP (100 $\mu\text{g}/\text{mouse}$, intraperitoneal injection 1 h before N-protein administration). Lung tissue and BAL samples were collected at 24 h after N-protein insult. (A) Tissue sections were stained with H&E (n = 3). (B) Total protein, total cells, and neutrophils in the BAL were determined to evaluate lung injury (n = 8). (C) Levels of IL-1 β , IL-6, and TNF- α in the BAL were analyzed via ELISA (n = 8). Data are presented as mean \pm SD. **p < 0.01, *** p < 0.001. One-way AVOVA with Tukey's post hoc test (B-C). n: number of independent experiments.

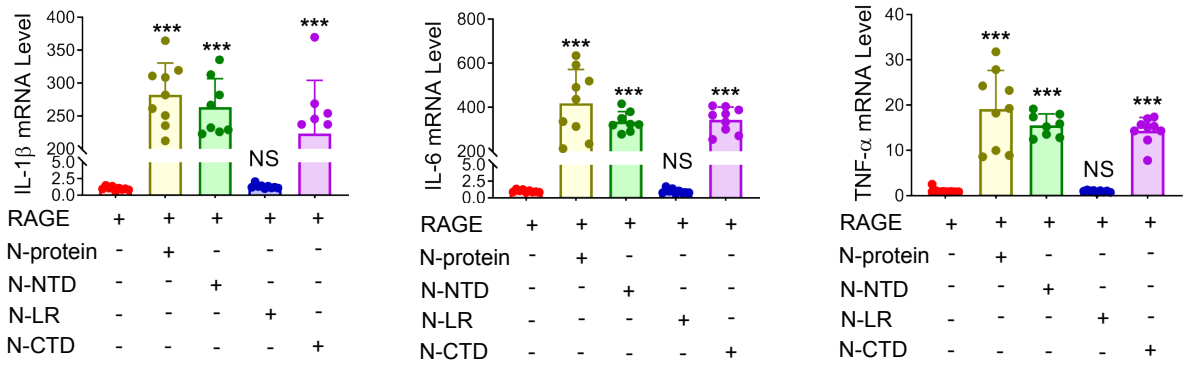




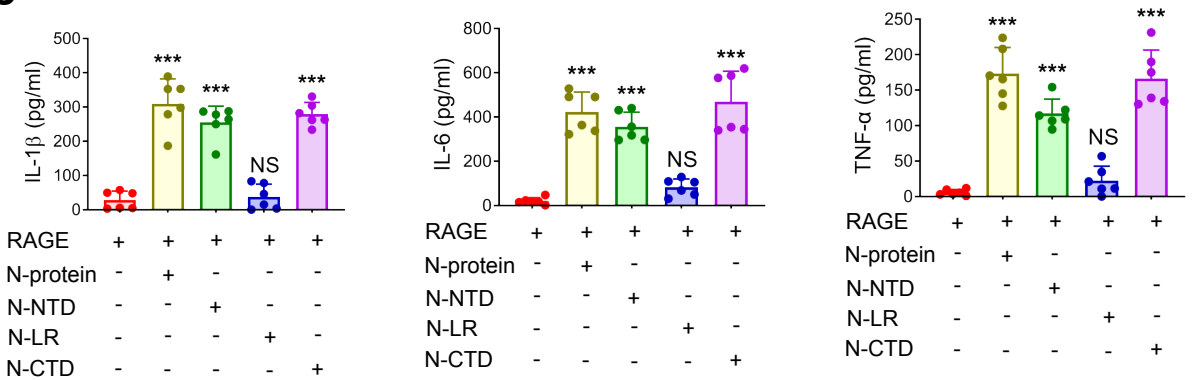
A

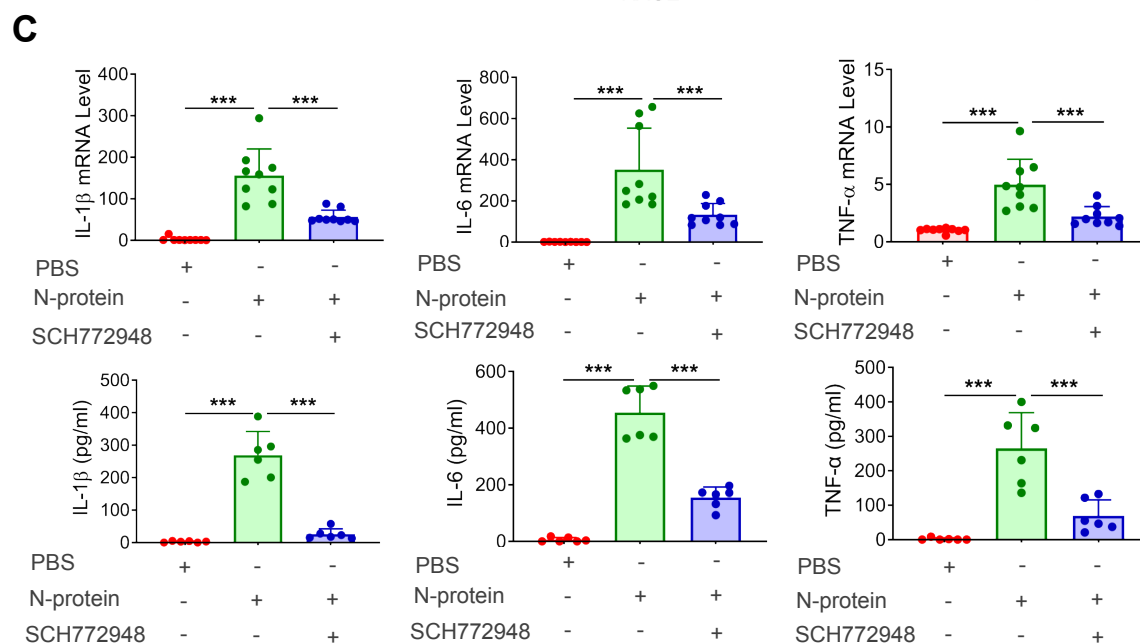
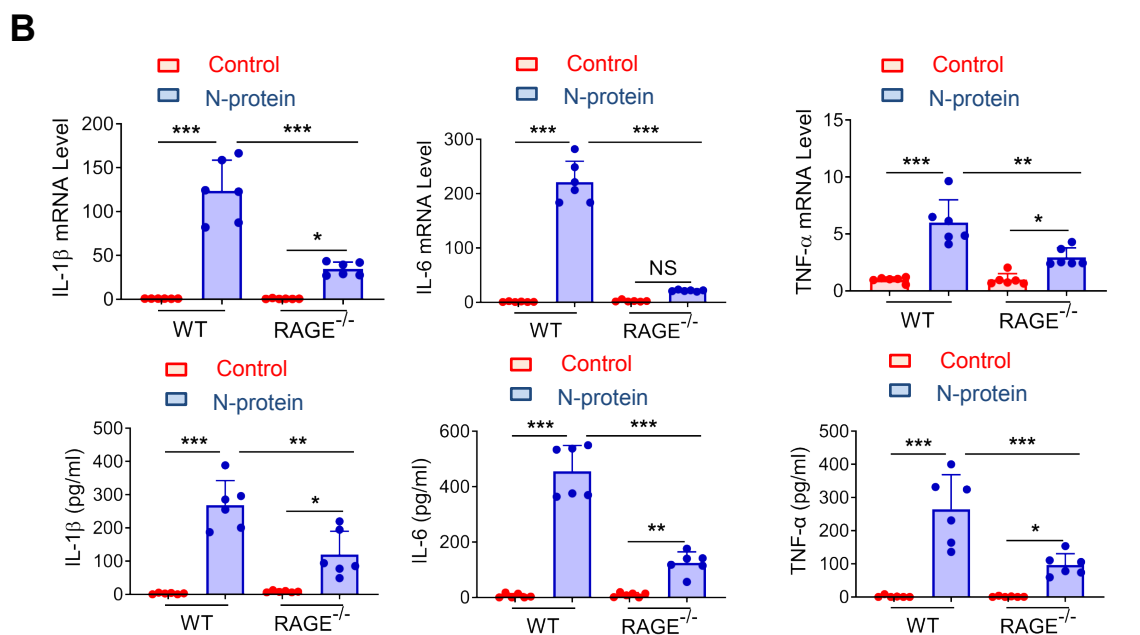
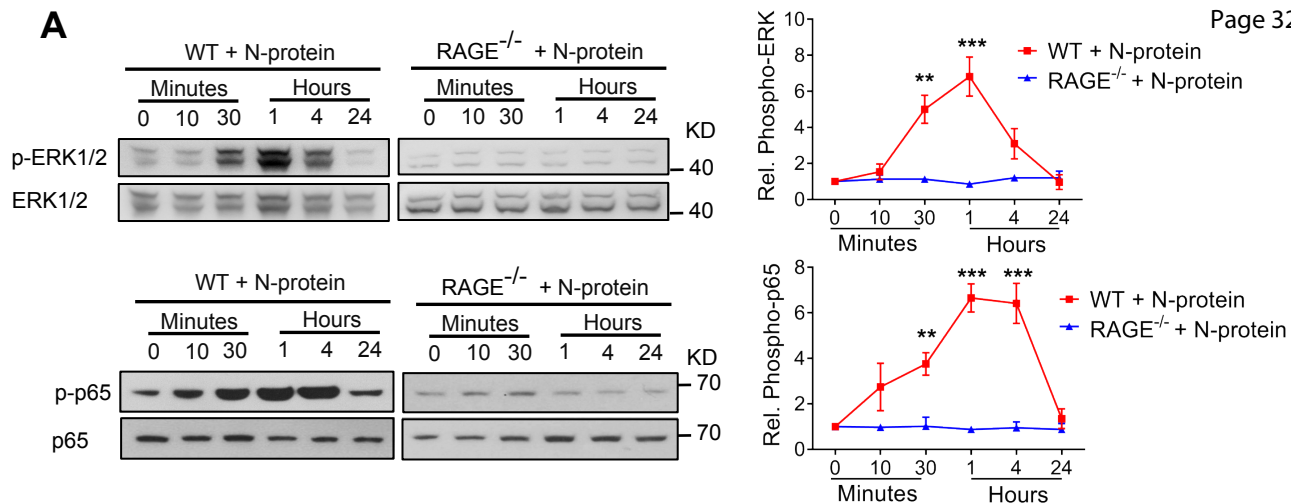


B

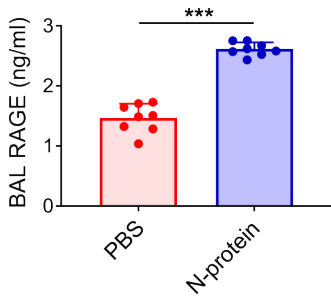


C

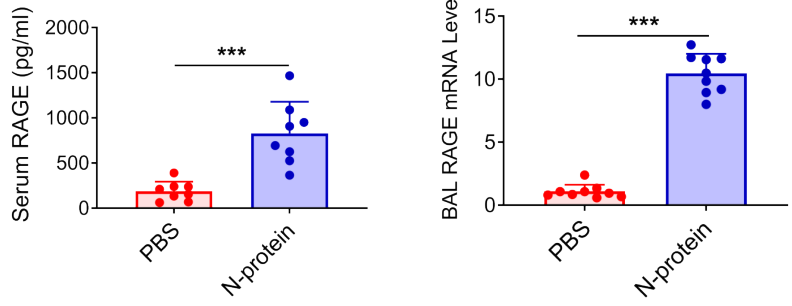




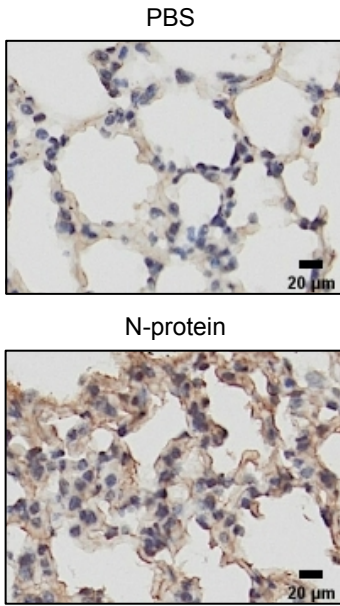
A



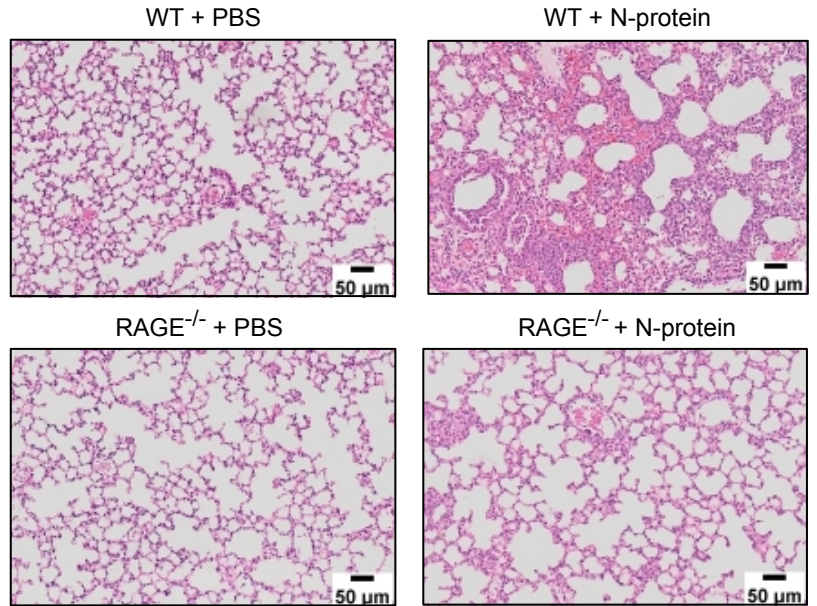
B



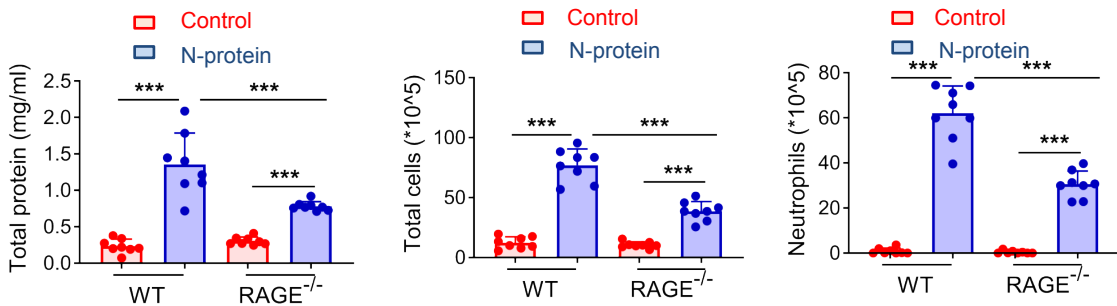
C



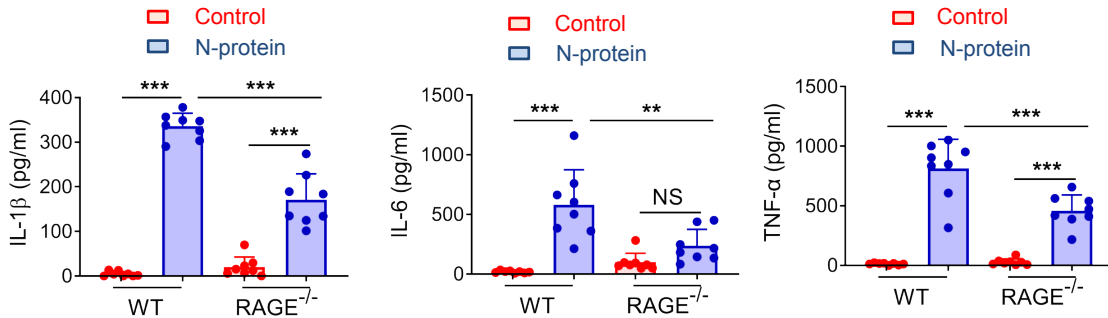
D

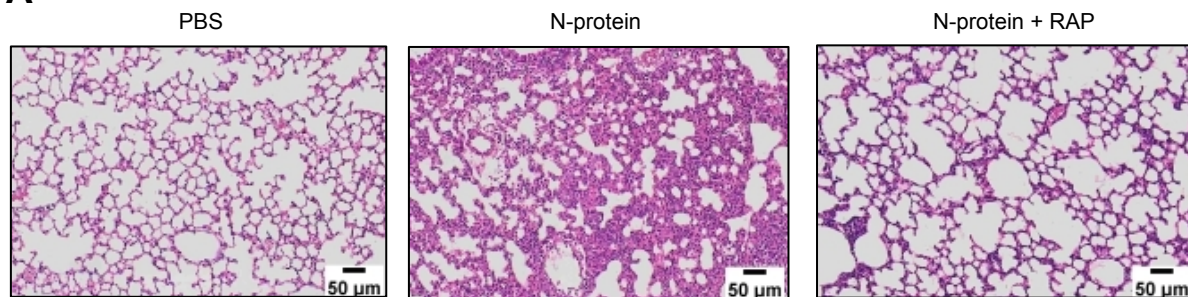
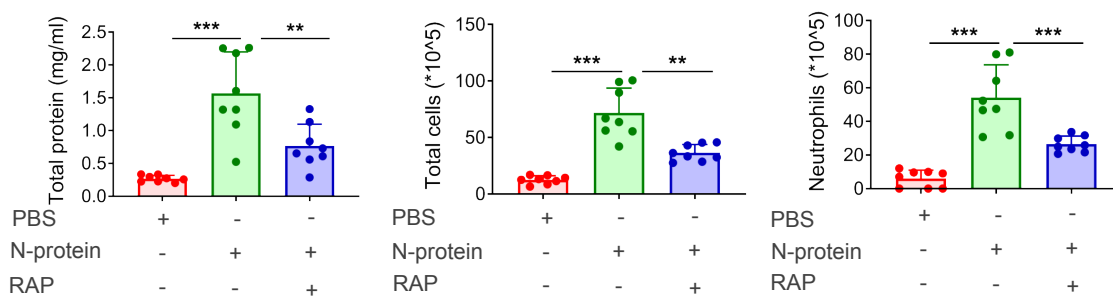
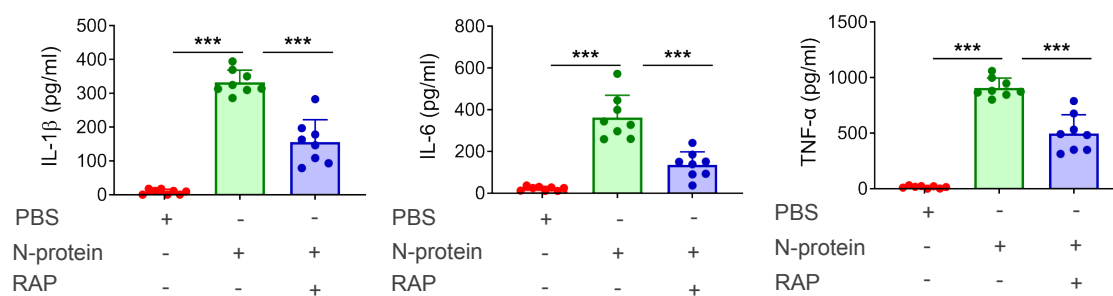


E



F



A**B****C**

RAGE is a receptor for SARS-CoV-2 N protein and mediates N protein-induced acute lung injury

Jie Xia, Jiangmei Wang, Liyang Ying, Ruoqiong Huang, Kai Zhang, Ruoyang Zhang, Wenqi Tang, Qi Xu, Dengming Lai, Yan Zhang, Yaoqin Hu, Xiaodie Zhang, Ruoxi Zang, Jiajie Fan, Qiang Shu, Jianguo Xu

ONLINE DATA SUPPLEMENT

Methods

Plasmids and fusion proteins

N-protein N-terminal domain (NTD, 1-174 AA), linker region (LR, 175-246 AA), and C-terminal domain (CTD, 247-419 AA) constructs were amplified from a full-length N-protein cDNA via PCR, confirmed via sequencing, and subcloned into pcDNA3.1-GFP plasmid in frame for mammalian expression. Human RAGE cDNA construct was amplified from a full-length RAGE cDNA via PCR, confirmed via sequencing, and subcloned into pcDNA3.1-Flag plasmid. The construct for full-length pET28a-His-N-protein for bacterial expression was generously provided by Dr. Feng Cong from Guangdong Laboratory Animals Monitoring Institute. Recombinant His-protein constructs for NTD, LR, and CTD were amplified from a N-protein cDNA via PCR, confirmed via sequencing, and inserted into pET28a vector. Recombinant RAGE protein was purchased from SinoBiological (Beijing, China). The constructs for full-length pET28a-His-S100A8 and pET28a-His-S100A9 for bacterial expression were purchased from GenScript (Piscataway, NJ).

Cell culture, transfection, and treatment for HEK293 and RAW 264.7 cells

The HEK293 and RAW 264.7 cell lines were obtained from ATCC (Manassas, VA). Cells were maintained in DMEM supplemented with 10% fetal bovine serum (Biological Industries, Cromwell, CT) and 1x Penicillin/Streptomycin in a 37 °C, 5% CO₂ incubator. For transient transfection, HEK293 cells were cultured until ~60–80% confluency in 12-well plates. Then, 1 µg of DNA and 2 µl of Lipofectamine™ 3000 (Thermo Fisher, Waltham, MA) were mixed and added to 1 ml serum-free medium per well. Following a 12 h incubation, fresh medium was added to the culture plates. The cells were harvested 24 h post-transfection and lysed in a buffer containing 10 mM Tris-HCl, pH 7.4, 1 mM EDTA, 150 mM NaCl, 0.5% Nonidet P-40, 1 mM

Na₃VO₄, and 1 mM PMSF. The lysates were clarified by centrifugation at 14000 rpm for 15 min at 4 °C. The clarified supernatants were applied for co-immunoprecipitation and Western blot experiments. For treatment experiments, HEK293 and RAW 264.7 cell (5 x 10⁵ cells) were seeded in a standard 12-well plate and treated with N-protein (5 µg/ml) or PBS for different time periods. Alternatively, RAGE antagonist RAP (20 µM, MilliporeSigma, St. Louis, MO) or ERK inhibitor (SCH772948, 500 nM, Selleck Chemicals, Houston, TX) was added to the culture medium 1 h before N-protein treatment. Then, cells were collected for Western blot analysis at different time points and qRT-PCR analysis at 24 h. Culture supernatant at 24 h was analyzed for levels of interleukin (IL)-1β, IL-6, and tumor necrosis factor (TNF)-α via ELISA following manufacturer's instruction (Lianke Biotech, Hangzhou, China).

Preparation of recombinant N-protein

Plasmids for full-length and partial-length pET28a-His-N-proteins as well as S100A8 and S100A9 were transformed into competent *E. coli*. BL21 (DE3). A single colony of bacteria was inoculated into 10 mL LB medium with 50 µg/ml of kanamycin at 37 °C, with gentle shaking at 200 rpm for overnight. The culture was then applied to inoculate 1 liter of LB medium. When OD₆₀₀ of culture reached approximately 0.6, protein expression was induced by adding IPTG (BBI Life Sciences, Shanghai, China) at 1 mM for 4 h. The proteins were purified from bacterial lysate via nickle affinity chromatography (BBI Life Sciences) and dialyzed to remove extra salt and imidazole. To remove the contaminated endotoxin, the recombinant proteins were passed through a column from ToxinEraser Endotoxin Removal Kit (GenScript). The endotoxin levels were < 0.1 EU/µg protein (<0.01 ng/µg) as determined by ToxinSensor Chromogenic LAL Endotoxin Assay Kit (GenScript). To neutralize the possible protein-bound LPS, recombinant proteins were pretreated with polymyxin B (250 µg/ml, MilliporeSigma) for 1 h at room

temperature (RT) before all in vitro and in vivo experiments.

Isolation and treatment of mouse bone marrow-derived macrophages (BMDMs)

Bone marrow was harvested from femurs and tibias of wild-type C57BL/6 and RAGE knockout mice. Cell clumps were dispersed with a 10 ml syringe attached with a 19-gauge needle. Then, cells were harvested via centrifugation and incubated with 1x lysis buffer (10 mM KHCO₃, 155 mM NH₄Cl, 0.1 mM EDTA) for 3 min to lyse red blood cells. Cells were pelleted again and differentiated in DMEM supplemented with GM-CSF (20 ng/ml, PeproTech, Rock Hill, NJ), 10% fetal bovine serum for 7 days. BMDMs (5 x 10⁵ cells) were seeded in a standard 12-well plate and treated with N-protein (5 µg/ml) or PBS for different time periods. For ERK1/2 inhibition experiment, BMDMs from wild-type C57BL/6 mice were pretreated with ERK inhibitor (SCH772948, 500 nM) for 1 h before adding N-protein (5 µg/ml). Cells were collected for Western blot at different time points and qRT-PCR analysis at 24 h. Culture supernatant at 24 h was analyzed for levels of IL-1β, IL-6, and TNF-α via ELISA .

Flow cytometry-based binding assay

For flow cytometry, A549 cells and BMDMs were detached by cell scrapers and rinsed with flow cytometry buffer (PBS, 0.5 % BSA) to block non-specific binding. Cells were then incubated with His-tagged full-length N-protein (5 µg/ml) at 37 °C for 1 h. Cells were washed with flow cytometry buffer for 3 x 5 min and incubated with an Alexa Fluor 488-conjugated anti-His antibody (Biolegend, San Diego, CA) diluted 1:100 for 30 min. Then, cells were rinsed and resuspended with flow cytometry buffer for detection of protein bound to A549 cells and BMDMs. Data were collected by a BD LSRFortessa™ flow cytometer and analyzed using FlowJo V10 software.

Pull-down assay

Pull-down assay was performed per the instruction of Pierce Pull-Down PolyHis Protein: Protein Interaction Kit (Thermo Fisher). “Baits” were His-tagged proteins expressing full-length, NTD, LR, and CTD. “Prey” was lung lysate from 6 to 8-week-old C57/BL6 mice. Briefly, purified His-tagged bait proteins were immobilized to cobalt chelate column by incubation for 1 h at 4 °C. Prey proteins from lung lysate were captured by applying to the column and incubated at 4 °C with gentle shaking for 2 h. Bait–prey protein complexes were eluted by the elution buffer with 290 mM imidazole. The eluted proteins were resolved on 12% sodium dodecyl sulfate polyacrylamide gel electrophoresis (SDS-PAGE) and detected by Western blot with a rabbit anti-RAGE antibody (Abcam, Waltham, MA).

Immunoprecipitation

After transient transfection for 24 h, cell lysates were prepared in lysis buffer (10 mM Tris-HCl, pH 7.4, 1 mM EDTA, 150 mM NaCl, 0.5% Nonidet P-40, 1 mM Na₃VO₄, and 1 mM PMSF). Protein concentrations in cell lysates were determined using a BCA protein assay kit (Thermo Fisher), exhibiting strong absorbance at 562 nm. An aliquot of lysates was saved as Input. The rest of the lysates (500 µg) was subjected to incubation with anti-Flag M2 affinity gel (MilliporeSigma) at 4 °C for 2 h with gentle end-over-end rotation. After 5 washes with lysis buffer, the bound proteins were eluted from the beads with SDS-PAGE sample buffer. The cell lysates and immunoprecipitation fractions were loaded onto SDS-PAGE gels after boiling for 5 min and subjected to Western blot analysis with an anti-GFP antibody (Abcam) or anti-Flag antibody.

Surface plasmon resonance (SPR)

To determine the specific affinity of real-time binding between N-protein and RAGE, SPR was performed using a Biacore 3000 system (Cytiva, Marlborough, MA). N-protein was diluted

in PBS to generate a series of concentrations (6.25-400 nM). After immobilizing RAGE at 100 RU level on the surface of a CM5 sensor chip (Cytiva) using amine coupling procedure, N-protein samples at concentrations of 400, 200, 100, 50, 25, 12.5 and 6.25 nM were injected for 4 min across the sensor surface at a flow rate of 20 μ L/min. At the end of the sample injection, PBS was flowed over the sensor surface for 4 min to promote dissociation. The response was monitored as a function of time at RT. After each analytic injection, sensor surface was regenerated with 1 min injection of 10 mM glycine-HCl (pH 2.5). Sensorgrams were obtained by subtraction of zero concentration curve. The binding data was fitted to a 1:1 binding model using BIAevaluation software (Cytiva).

ELISA assay for EC₅₀

ELISA plates were coated with His-tagged full-length N-protein (1 μ g/ml) alongside negative control wells with 100 μ L PBS. Plates were incubated overnight at 4 °C and washed with 0.05% v/v Tween-20 in PBS (PBS-T) for 3 times. The plates were then blocked with blocking buffer (3% BSA in PBS) at RT for 1 h and washed with PBS-T for 3 times. Blocked wells were incubated with a series of concentrations of RAGE (0.1 - 25.6 μ g/ml) or PBS in a volume of 100 μ L/well for 1 h at 37°C. Wells were then rinsed 3 times with PBS-T and incubated 1 h at RT with 100 μ L of a rabbit anti-RAGE antibody diluted 1:1000 in blocking buffer. After washing 3 times with PBS-T, wells were incubated for 1 h at RT with 100 μ L of a goat anti-rabbit antibody conjugated to horseradish peroxidase (Abcam) diluted 1:5000 with blocking buffer. After another washing 3 times with PBS-T, 100 μ L/well 3,3',5,5'-tetramethylbenzidine (TMB) substrate was added to each well and incubated for 30 min at RT in the dark. Absorbance was read at 450 nm with SpectraMax 190 Microplate Reader (Molecular Devices, San Jose, CA) after the reaction was terminated by adding 100 μ L of 2 N HCl. The

EC₅₀ value was calculated from linear regression analysis.

N-protein-induced lung injury model

C57BL/6 mice (6-8 weeks old) were acquired from Shanghai Laboratory Animal Center (Shanghai, China). RAGE knockout mice with C57BL/6 background was generated by Nanjing Biomedical Research Institute of Nanjing University via CRISPR/Cas9 technology (Project#: XM709828). All animals were kept in cages at a temperature-controlled facility of the Zhejiang University Laboratory Animal Center. Animal experimental protocols were approved by the Institutional Animal Care and Use Committee at Zhejiang University School of Medicine. All mice were simultaneously assigned into the treatment groups in a random order. Mice were anesthetized with an injection of phenobarbital (50 mg/kg) intraperitoneally. Acute lung injury was induced via intratracheal instillation of recombinant full-length N-protein (75 µg per mouse in 50 µL). To study the effect of RAGE inhibition on N-protein-induced lung injury, mice were subjected to intraperitoneal injection of RAGE antagonist RAP (50 or 100 µg/mouse) 1 h before N-protein administration. To study the effect of NLRP3 inhibition on N-protein-induced lung injury, mice were treated with intraperitoneal injection of MCC950 (10 mg/kg, Selleck Chemicals, Houston, TX) 1 h before N-protein administration. Based on our experience, the optimal time point for assessing N-protein-induced lung injury was 24 h after insult. Serum, lung, and bronchioalveolar lavage (BAL) samples were harvested at 24 h from mouse groups (BAL samples were harvested at 48 h in Supplemental Figure 1). RAGE levels in serum and BAL were determined by ELISA (Lianke Biotech). Total RAGE mRNA expression in BAL cells was examined via qRT-PCR.

Inflammatory cell counts, protein, and cytokines in BAL

Mice were anesthetized with an injection of phenobarbital (50 mg/kg) intraperitoneally. To

obtain BAL from mice, the tracheas were cannulated with 18G blunt-end needles and the lungs were flushed with 0.5 ml of cold PBS for 3 times. BAL was centrifuged for 5 min at 400 x g at 4 °C to collect the pellet and supernatant. The cell pellet was resuspended with PBS and enumerated for total white blood cell counts using a hemocytometer. An FITC-conjugated anti-mouse Ly-6G (Gr-1) antibody (Thermo Fisher) was applied to examine the percentage of neutrophils in the BAL via flow cytometry. Total neutrophil counts in the BAL were calculated by multiplying the percentage of neutrophils by the total counts of white blood cells. Protein level in the BAL supernatant, an index of lung capillary permeability, was examined using a Pierce BCA Protein Assay Kit (Thermo Fisher). BAL supernatant was also measured for cytokines including IL-1 β , IL-6, and TNF- α via ELISA per manufacturer's protocol.

Histopathology

Lung tissue pathology was performed on mice without lavage. To harvest the lungs for histological analysis, the trachea was cannulated with a 18G blunt-end needle and the lungs inflated with 1 ml of 4% buffered paraformaldehyde. After fixation for 24 h, the lungs were processed in a tissue processor overnight, embedded in paraffin, and cut at 5 μ m in thickness. After deparaffinization and rehydration, lung sections were then stained with hematoxylin and eosin (H&E) to examine cellular and morphological structures. RAGE expression in lung tissue was examined using a Vectastain ABC elite kit (Vector Laboratories, Newark, CA)). Briefly, deparaffined sections were treated with 0.3% hydrogen peroxide for 30 min to quench endogenous peroxidase activity. Sections were then incubated with rabbit anti-RAGE antibody (Abcam) for 30 min at room temperature. After that, the sections were rinsed with PBS and probed with biotinylated secondary antibody for 30 min. After washing with PBS again, sections were incubated with ABC reagent for 30 min and peroxidase substrate solution for 1 min.

Finally, the sections were counterstained with hematoxylin, cleared with alcohol-xylene, and mounted.

Western blot

Cells seeded in 12-well cluster plates were harvested and lysed in cell lysis buffer. The protein concentration of cell lysates was examined using BCA protein assay. Equal amount of cell lysates (30 μ g) were separated on 12% SDS-PAGE gels, transferred via polyvinylidene fluoride membranes (Millipore, Billerica, MA), blocked in tris-buffered saline with Tween-20 (TBST) containing 5% non-fat milk (blot buffer), and probed with the primary antibodies to phosphor-ERK1/2 (ab76299, Abcam), ERK1/2 (ab184699, Abcam), phosphor-JNK1/2 (#4668, Cell Signaling Technology, Danvers, MA), JNK1/2 (#9252, Cell Signaling Technology), phosphor-p38 (#4511, Cell Signaling Technology), p38 (#8690, Cell Signaling Technology), phosphor-NF- κ B p65 (#3033, Cell Signaling Technology), and NF- κ B p65 (#8242, Cell Signaling Technology). After washing with blot buffer, membranes were incubated with specific secondary antibodies linked to horseradish peroxidase (Thermo Fisher). Signal detection was conducted using enzyme-linked chemiluminescence kit (Biological Industries, Kibbutz Beit-Haemek, Israel). Blot images were analyzed by ImageJ software.

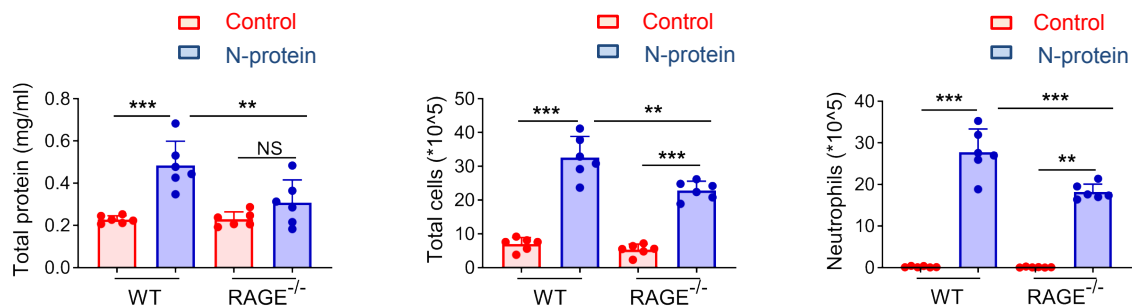
Quantitative real-time PCR (qRT-PCR)

Cells were extracted for total RNA with Trizol reagent (Thermo Fisher) following the manufacturer's instructions. The concentration of RNA samples was examined with a Nanodrop Spectrophotometer (ND-2000; Thermo Fisher). RNA (1 μ g) was reversely transcribed to cDNA using Primescript RT reagent kit (Takara Bio, Kusatsu, Japan). cDNA template was amplified using TB Green Premix Ex Taq II (Takara Bio). mRNA raw data (C_t) were normalized to the levels of β -actin mRNA to allow comparisons between samples and expressed as fold change

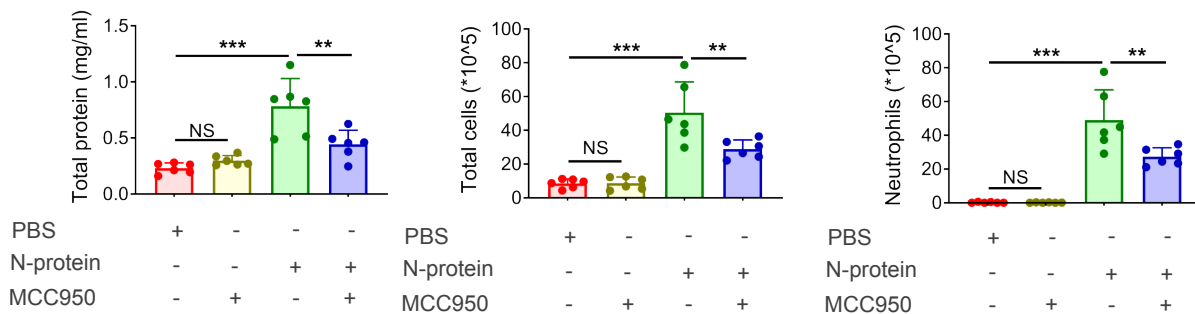
relative to control sample. The sequences of PCR primer pairs were the following: IL-1 β forward 5'GAAATGCCACCTTTTGACAGTG3', reverse 5'TGGATGCTCTCATCAGGACAG3'; IL-6 forward 5'CTGCAAGAGACTTCCATCCAG3', reverse 5'AGTGGTATAGACAGGTCTGTTGG3'; TNF- α forward 5'CAGGCGGTGCCTATGTCTC3', reverse 5'CGATCACCCCGAAGTTCAGTAG3'; RAGE forward 5'CTTGCTCTATGGGGAGCTGTA3', reverse 5'CATCGACAATTCCAGTGGCTG3'; β -actin forward 5'CGTTGACATCCGTAAAGACC3', reverse 5'AACAGTCCGCCTAGAAGCAC3'.

Statistical methods

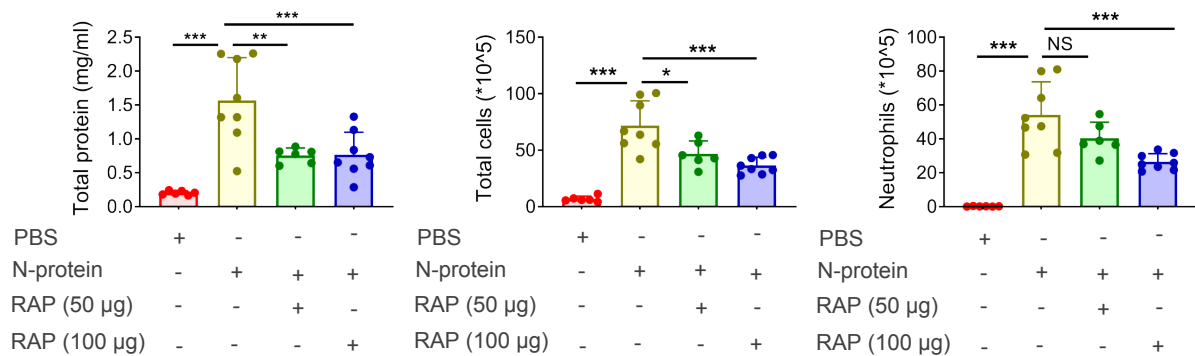
Data are presented as mean \pm standard deviation of the mean (SD). Data normality was examined using the D'Agostino-Pearson Omnibus normality test, the Shapiro-Wilk normality test, or Kolmogorov-Smirnov test with Dallal-Wilkinson-Lilliefors corrected p value. Student's t test, one-way analysis of variance (ANOVA) with Tukey's post hoc test, or two-way ANOVA with Tukey's post hoc test was conducted for parametric values. In data sets with non-parametric values (Figure 2F and TNF- α of Figure 3B), Kruskal-Wallis test followed by Dunn's post hoc test was performed for analysis. Statistical analysis was conducted using the GraphPad Prism 8.0.2. Results were deemed significant if $p < 0.05$.



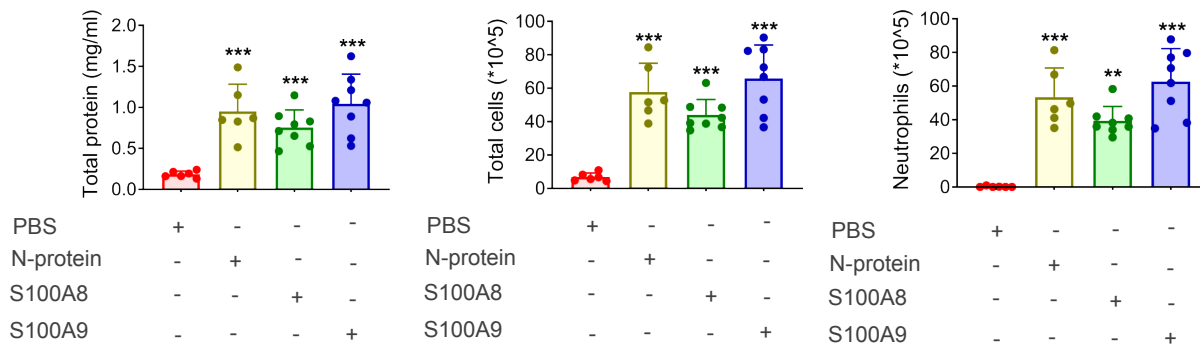
Supplemental Figure 1. Effect of RAGE deficiency on N-protein-induced acute lung injury at 48 h after N-protein insult. RAGE^{-/-} mice with C57BL/6 background and WT C57BL/6 mice were treated with PBS or N-protein (75 μ g/mouse in 50 μ l) intratracheally. BAL samples were collected at 48 h after N-protein insult. Total protein, total cells, and neutrophils in the BAL were assayed to evaluate lung injury (n = 6). Data are presented as mean \pm SD. **p < 0.01, ***p < 0.001. Two-way AVOVA with Tukey's post hoc test. NS: not significant. n: number of independent experiments.



Supplemental Figure 2. Effect of NLRP3 inhibitor MCC950 on N-protein-induced acute lung injury. C57BL/6 mice were treated with PBS, MCC950 intraperitoneally (10 mg/kg, 1 h before N-protein treatment), N-protein (75 μ g/mouse in 50 μ l) intratracheally, or MCC950 + N-protein. BAL samples were collected at 24 h after N-protein insult. Total protein, total cells, and neutrophils in the BAL were assayed to evaluate lung injury (n = 6). Data are presented as mean \pm SD. **p < 0.01, ***p < 0.001. One-way AVOVA with Tukey's post hoc test. NS: not significant. n: number of independent experiments.



Supplemental Figure 3. Effect of different doses of RAGE antagonist on N-protein-induced acute lung injury. WT C57BL/6 mice were treated with PBS, full-length N-protein (75 µg/mouse), N-protein + RAGE antagonist RAP (50 µg/mouse, intraperitoneal injection 1 h before N-protein administration), or N-protein + RAGE antagonist RAP (100 µg/mouse). BAL samples were collected at 24 h after N-protein insult. Total protein, total cells, and neutrophils in the BAL were determined to evaluate lung injury. Data are presented as mean ± SD, n = 6-8. *p < 0.05, **p < 0.01, *** p < 0.001. One-way ANOVA with Tukey's post hoc test. NS: not significant. n: number of independent experiments.



Supplemental Figure 4. Comparison the effects of S100A8, S100A9, and N-protein on acute lung injury. Recombinant His-tagged S100A8 and S100A9 proteins were prepared as N-protein. C57BL/6 mice were treated with PBS, N-protein (75 $\mu\text{g}/\text{mouse}$ in 50 μl), S100 A8 (75 $\mu\text{g}/\text{mouse}$ in 50 μl), or S100 A9 (75 $\mu\text{g}/\text{mouse}$ in 50 μl) intratracheally. BAL samples were collected at 24 h after insult. Total protein, total cells, and neutrophils in the BAL were assayed to evaluate lung injury (n = 6-8). Data are presented as mean \pm SD. **p < 0.01, ***p < 0.001 versus PBS control. One-way AVOVA with Tukey's post hoc test. n: number of independent experiments.